Title
Biomarkers in CNS-originating Extracellular Vesicles for Parkinson's disease and Multiple System Atrophy

Author
Taha, Hash Brown

Publication Date
2023

Peer reviewed|Thesis/dissertation

UNIVERSITY OF CALIFORNIA

Los Angeles

Biomarkers in CNS-originating Extracellular Vesicles for Parkinson's disease and Multiple System Atrophy

A thesis submitted in partial satisfaction of the requirements for the degree Master of Science in Physiological Science

by

Hash Taha

2023

ABSTRACT OF THE THESIS

Biomarkers in CNS-originating Extracellular Vesicles for Parkinson's disease and Multiple System Atrophy

by

Hash Taha

Master of Science in Physiological Science

University of California, Los Angeles, 2023

Professor Ketema N. Paul, Committee Co-Chair

Professor Kacie Danielle Deters, Committee Co-Chair

Synucleinopathies are a group of neurodegenerative diseases including Parkinson's disease (PD), dementia with Lewy bodies (DLB), and multiple system atrophy (MSA). These diseases are characterized by the aggregation and deposition of α-synuclein (α-syn) in Lewy bodies (LBs) in PD and DLB or as glial cytoplasmic inclusions in MSA. Current antemortem differential diagnosis of Parkinson's disease (PD) and multiple system atrophy (MSA) is challenging due to the overlap of Parkinsonian symptoms, especially in the early stages. Analysis of biomarkers in CNS-originating extracellular vesicles (EVs) isolated from blood is a promising strategy for these diseases. EVs are released by all cell types and pass through the blood-brain barrier, providing a proxy of the brain's biochemistry. We have shown previously that α-synuclein (α-syn) concentration in neuronal- and oligodendroglial-EVs (nEVs and oEVs, respectively) isolated from the serum or plasma of healthy controls (HC), and patients with PD or MSA allowed separating MSA from both HC and PD with high sensitivity and specificity. In healthy brains, only ~4% of α-syn is phosphorylated at Ser129 (pS129-α-syn), whereas >90% pS129-α-

syn may be found in LBs, suggesting that pS129-α-syn could be a helpful biomarker for synucleinopathies. Further, tau is implicated in patients with PD but not MSA. Here, I describe the development of a novel electrochemiluminescence ELISA for the measurement of pS129-α-syn in nEVs and oEVs based on the Meso Scale Discovery platform. Using this in-house assay and other commercial assays, we measured α-syn phosphorylated at Ser 129 (pS129-α-syn), total tau, and neurofilament light chain (NfL) in subsets of patients with PD, MSA or HCs to test if they improved the diagnostic power.

The findings may suggest that a biomarker panel compromising nEVs α-syn, oEVs:nEVs α-syn, oEVs pS129-α-syn and exosome concentration may help distinguish patients with PD from MSA. However, many limitations currently exist with issues related to preanalytical variables, the need for independent validation and replication, differing postmortem diagnosis from the antemortem diagnosis, assay matrix effects, and issues with the L1CAM antibody, among others. Several notable limitations are associated with the current state of research in this area. These limitations encompass various factors such as preanalytical variables, the necessity for independent validation and replication, discrepancies between postmortem and antemortem diagnoses, assay matrix effects, challenges related to the L1CAM antibody, and other related issues.

The thesis of Hash Taha is approved.

Xia Yang

Kacie Danielle Deters, Committee Co-Chair

Ketema N. Paul, Committee Co-Chair

University of California, Los Angeles

2023

Dedication

Engraved on the tapestry of my life is the tale of my mother, an extraordinary woman whose resilience and strength has been the cornerstone of our family. She lost both her parents at an early age, yet despite life's early cruelty, she persevered, juggling more than full-time work and high school, failing and rising again four times until she finally graduated. Her story took a different turn when she found love with my father, but their time together was short-lived, as he departed from this world when I was merely two years old. In the face of daunting adversity as a foreigner, my mother single-handedly took the reins of raising five children. With grit and grace, she worked long hours to ensure we had our needs met. She became the epitome of resilience, with not a single complaint escaping her lips nor a tear tarnishing her always bright-eyed smile. In addition, she exhibited unwavering care and devotion to my brother, who tragically suffers from brain atrophy due to oxygen deprivation as a toddler. Yet life had another trial for her; she was diagnosed with Parkinson's disease. Even as she battles this condition as a consequence of REM sleep behavior disorder conversion, she continues to amaze us all with her spirit and tenacity. Every hurdle she has faced, every challenge she continues to tackle, is done so with an inspiring sense of fortitude and optimism.

Amidst her ceaseless struggles, she never let the hardships dilute her belief in education. As a testament to her wisdom, she ceaselessly emphasized the transformative power of higher education to us, her children. Her life, defined by her unyielding resilience, boundless love, and enduring spirit, has been my most significant source of inspiration. **I dedicate this work to my mother. I am most grateful to her.**

Table of Contents

Chapter 1

Chapter 2

List of figures

Chapter 1

Chapter 2

Acknowledgments

I would like to extend my deepest gratitude to all those who have supported my journey to this point. I am particularly thankful for the Department of Integrative Physiology at the University of Colorado Boulder, whose enduring support, nurturing environment, and boundless opportunities have been crucial in my academic and personal development. I owe a special debt of gratitude to Ruth Heisler, Heidi Bustamante, and Steven Hobbs, who have generously shared their wisdom and time, and whose guidance has been indispensable. The opportunities they have given me were fundamental in my success. Furthermore, I appreciate the trust placed in me by Jennifer Martin, Bradley Olwin, Alicia Cutler and Celine Vetter. Their belief in my capabilities allowed me to gain invaluable experience through undergraduate research, which significantly enriched my master's program. I also thank Robert Spencer for his support and understanding during my undergraduate neuroscience education. I am also immensely thankful to Kenneth Wright and Brandon Michieli for their exceptional support and responsiveness during an extraordinarily difficult phase of my life. Their unwavering assistance was a tremendous source of strength and improved my mental health substantially. I am immensely grateful for their unwavering support.

I am profoundly grateful for the continued support and guidance provided by the Integrative Biology & Physiology Department at UCLA. I extend my deepest gratitude to our esteemed M.S. Director and Vice-Chair of the department, Dr. Amy Rowat, whose leadership, wisdom, and unwavering belief in my potential have shaped my academic journey significantly. I am equally indebted to my committee members, Dr. Ketema Paul, Dr. Kacie Deters, and Dr. Xia Yang. Their invaluable feedback, insightful critique, and persistent encouragement have enabled me to navigate challenges with grace and fortitude, and their fairness and justice in all matters

have instilled a deep sense of trust and respect in me. On multiple occasions, Drs. Paul and Deters provided me with critical advice and offered 1-on-1 meetings to help with ongoing issues. For that, I'm extremely grateful.

Finally, my sincere appreciation also goes to Marisela Diaz-Vasquez, our student advisor. Her dedication to our success is truly remarkable, and her genuine care has made a profound impact on my academic experience. I and other students in the program greatly appreciate her warm support and unwavering willingness to help.

Each of these individuals (and many others) has contributed to my personal and professional growth, and for this, I am eternally thankful.

The materials presented in Chapter 1 and Chapter 2 are published under a CC BY 4.0 open access license at ACS Chemical Neuroscience, Translational Neurodegeneration and Frontiers in Neurology, which allows redistributions of the material. I am grateful for the invaluable assistance provided by my co-authors, especially Leony Fenwick, Suman Dutta, Simon Hornung and Lea Chamoun, who played a crucial role in making this work possible. The contributions of each co-author are outlined in the contribution section of each peer-reviewed manuscript.

Chapter 1

Development of a novel electrochemiluminescence ELISA for quantification of α-synuclein phosphorylated at Ser^{129} in biological samples.

Expanded Version.

ACS Chemical Neuroscience

Publication Date: March 15th, 2023

https://doi.org/10.1021/acschemneuro.2c00676

ABSTRACT

Synucleinopathies are a group of neurodegenerative diseases including Parkinson's disease (PD), dementia with Lewy bodies (DLB), and multiple system atrophy (MSA). These diseases are characterized by the aggregation and deposition of α-synuclein (α-syn) in Lewy bodies (LBs) in PD and DLB or as glial cytoplasmic inclusions in MSA. In healthy brains, only ~4 % of α-syn is phosphorylated at Ser^{129} (pS^{129}-α-syn), whereas > 90% pS^{129}-α-syn may be found in LBs, suggesting that pS^{129}-α-syn could be a useful biomarker for synucleinopathies. However, a widely available, robust, sensitive, and reproducible method for measuring pS^{129}-α-syn in biological fluids is currently missing. We used Meso Scale Discovery (MSD)'s electrochemiluminescence platform to create a new assay for sensitive detection of pS^{129}-α-syn. We evaluated several combinations of capture and detection antibodies and used semi-synthetic pS^{129}-α-syn as a standard for the assay at a concentration range from 0.5 to 6.6×10^4 pg/mL. Using the antibody EP1536Y for capture and an anti-human α-syn antibody (MSD) for detection was the best combination in terms of assay sensitivity, specificity, and reproducibility. We tested the utility of the assay for the detection and quantification of pS^{129}-α-syn in human cerebrospinal fluid, serum, plasma, saliva, and CNS-originating small extracellular vesicles, as well as in mouse brain lysates. Our data suggest that the assay can become a widely used method for detecting pS^{129}-α-syn in biomedical studies including when only a limited volume of sample is available and high sensitivity is required, offering new opportunities for diagnostic biomarkers, progression, and quantifying outcome measures in clinical trials.

Introduction

Synucleinopathies, including Parkinson's disease (PD), dementia with Lewy bodies (DLB), and multiple system atrophy (MSA) are characterized clinically by a chronic and progressive decline in motor, cognitive, behavioral, and/or autonomic functions. Deposits of fibrillar α-synuclein (α-syn) as Lewy bodies (LBs) and Lewy neurites in PD and DLB, or as glial cytoplasmic inclusions (GCIs) in MSA, are pathological hallmarks of these diseases [1, 2]. Differential diagnosis of synucleinopathies is difficult due to clinical symptoms overlap, especially in early disease stages [3]. Phosphorylated forms of α-syn, particularly at Ser129 (pS^{129}-α-syn) are highly enriched in LBs and GCIs and are thought to be related to the disease process [4, 5]. Therefore, if pS^{129}-α-syn can be measured in bodily fluids of patients it could serve as a sensitive biomarker for improving diagnosis accuracy, measuring disease progression, and assessing therapeutic outcomes [6, 7].

Currently, commercially available assays for quantifying pS^{129}-α-syn are limited. Cell-based ELISAs are available from Abexxa (Cambridge, United Kingdom), Creative Diagnostics (Shirley, NY), and Aviva Systems Biology (San Diego, CA) yet based on the information provided by the companies, these assays are not optimized for detecting the recombinant protein in human samples available in limited quantities and suffer from intrinsically high variability, mainly due to the difficulty of plating the exact number of cells in each well, and to variation in cell proliferation rate and responsivity. A typical sandwich ELISA is sold by MyBioSource [8] yet the company's website disclaims: "cross-reaction to other targets may potentially exist" and, "cross-reactivity could vary between sample type or species". In addition, considering the low concentrations of pS^{129}-α-syn in human biofluid samples, as reported in earlier studies [9, 10] the

sensitivity limit of the assay, 3.12 ng/mL, likely would not allow reliable measurement in human biofluids.

Previously, several groups have reported assays for pS^{129}-α-syn, which varied widely in sensitivity, and used them to measure the phospho-protein in human cerebrospinal fluid (CSF) [11-13], plasma [12-14], human cell culture lysates [13], human and rat brain lysates [13], and human erythrocytes [15]. The assays included traditional ELISA [6, 11, 14] and higher-sensitivity methods, such as Singulex Erenna [12], Luminex [10] and AlphaLISA [13]. Recently, the Zhang group created a pS^{129}-α-syn electrochemiluminescence ELISA (ECLIA) using biotinylated anti-pS^{129}-α-syn (BioLegend, San Diego, CA) and anti-α-syn antibody clone 42 (BD Bioscience, CA) labeled with Sulfo-TAG. Applying this assay, they quantified the concentration of pS^{129}-α-syn in the membrane and cytosolic fractions of erythrocytes isolated from blood samples of healthy controls (HC) and patients with PD [15]. Despite the importance of pS^{129}-α-syn as a potential biomarker for diagnosis and measuring progression of synucleinopathies, none of these assays has become mainstream.

Three main issues likely have prevented the general use of the aforementioned assays. First, the specificity and reproducibility of the antibodies used varied and some of the antibodies were not readily available to other research groups. Second, in most of the studies published to date, the standard curve was generated using recombinant α-syn phosphorylated *in vitro* by casein kinase II [4, 6, 10, 11] or polo-like kinase 2 [13] raising concerns regarding the completion of the phosphorylation at Ser^{129} and possible phosphorylation of other sites, which might cross-react with the antibodies used in the assay or otherwise affect their binding to pS^{129}-α-syn [16].

Third, most studies published to date focused on demonstrating the suitability of their assays only for a specific sample type, e.g., CSF [10, 11] but did not report testing of different antibody

combinations, fine-tuning the protocol, or comparing the assay in different biofluids. To address these concerns, we have extensively researched publications on commercially available antibodies and used as a standard the semi-synthetic pS^{129}-α-syn first reported by the Lashuel group [17] and made available by the Michael J. Fox Foundation via Proteos Inc. We have considered multiple factors in selecting the antibodies, tested several methodological approaches, and evaluated the suitability of our assay to quantify pS^{129}-α-syn in several commonly analyzed biological sample types. A comparable study was published recently by Cariulo et al. in which they characterized different antibody combinations of anti-α-syn and anti-pS^{129} α-syn antibodies and measured total and pS^{129} α-syn in CSF and plasma using a Singulex Erenna immunoassay [12]. The novel ECLIA we describe here for measurement of pS^{129}-α-syn detects pg/mL concentrations of pS^{129}-α-syn and has a wide dynamic linear range and low intra- and inter-assay variability. It is suitable for use in multiple types of biological samples and thus provides a platform for measuring pS^{129}-α-syn as a biomarker for a variety of clinical and research applications.

Materials and Methods

Materials

Semi-synthetic pS^{129}-α-syn was obtained from Proteos Inc. (Kalamazoo, MI). Anti-pS^{129}-α-syn monoclonal antibody EP1536Y (ab209422) and anti-α-synuclein monoclonal antibody MJFR1 (ab138501) were procured from Abcam (Cambridge, UK). Small-spot streptavidin-coated 96-wells ELISA plates (L45SA), assay diluent (R50AM), recombinant human α-syn calibrator (C01WK), biotinylated anti-total α-syn antibody, SULFO-TAG anti-human α-syn antibody, GOLD SULFO-TAG NHS-Ester conjugation pack (R31AA) and read buffer (R92TC) were obtained from Meso Scale Discovery (Rockville, MD). Phosphate-buffered saline (PBS), Tris-

buffered saline (TBS), and biotin quantitation kit were from Thermo Fisher Scientific (Waltham, MA).

Biological samples

Pooled human serum and pooled human plasma were procured from Innovative Research (Novi, MI). Cerebrospinal fluid samples were collected postmortem from deceased patients with synucleinopathies or controls without a neurological disease whose diagnosis was determined by a neuropathological examination. The samples were obtained from from the UCLA Division of Neuropathology (2 PD, 2 DLB, 3 MSA), UC Irvine Institute for Memory Impairments and Neurological Disorders (MIND, 7 healthy controls), and Banner Sun Health Research Institute (BHSRI), Sun City, AZ (1 PD). Protocols for CSF collection postmortem were similar in the three institutions with small variations. At UCLA and BHSRI, CSF was drawn into 30-mL polypropylene syringes using 8-cm long 18-gauge needles. UCI MIND used similar needles but 20-mL syringes. At UCLA and BHSRI the CSF was transferred to 15-mL Falcon tubes and centrifuged at low speed to get rid of particulate matter. Then, the supernate was aliquoted into 0.5-mL aliquots. AT UCI MIND, the collected CSF was placed on ice until processing and then aliquoted into 0.25-mL aliquots. The aliquots in all three institutions were stored at –80 °C until use. Mouse brain extracts were from PLP-α-syn mice, a model of experimental MSA, or wild-type littermates, and were obtained as described previously [18]. All the biological samples were treated with 1X Halt™ Protease and Phosphatase Inhibitor Cocktail (Thermo Fisher Scientific).

Preparation of standard

The pS^{129}-α-syn standard was prepared according to the protocol published previously by Cariulo et al. [12]. Briefly, the lyophilized protein was weighed and dissolved in 100% trifluoroacetic acid (TFA) purchased from Alfa Aesar (Haverhill, MA). One µL of TFA was

added per 25 µg of protein. The TFA was evaporated completely in a fume hood for 1 h and the protein then was dissolved in TBS (50 mM Tris, 150 mM NaCl, pH 7.4) at a concentration of 20 µM. The solution was filtered through a 100-kDa cutoff filter from Pall (Show Low, AZ) and protein concentration was measured using a bicinchoninic acid (BCA) assay (Thermo Fisher Scientific). 1% (v/v) Tween-20 (Fisher BioReagents, Pittsburgh, PA) was added and the solution was aliquoted and stored at –80 °C.

Biotinylation and sulfonation of antibodies

For biotinylation of antibody EP1536Y, 40 µL of a 0.90-mg/mL solution of the antibody were incubated with 1.61 µL of 11 mM Sulfo-NHS-Biotin (50-fold molar excess) on ice for 2 h according to the manufacturer's protocol (EZ-Link™ Micro Sulfo-NHS-LC-Biotinylation Kit, Thermo Fisher Scientific). Excess free biotin was removed using a 0.5-mL 7-kDa MWCO Zeba™ Spin Desalting Column (Thermo Fisher Scientific). Two hundred µL of ultra-pure water (purified using a Milli-Q system, Millipore, Burlington, MA) were added as a stacker volume for elution of the biotinylated EP1536Y antibody. Forty µL of 1.167-mg/mL solution of antibody MJFR1 were biotinylated using the same biotinylation kit. Biotinylation levels were evaluated using a fluorescence biotin quantitation kit (Thermo Fisher Scientific). For sulfonation, 40 µL of a 0.90-mg/mL of EP1536Y solution were incubated with SULFO-TAG NHS-Ester (MSD) according to the manufacturer's instructions. The protein concentration of all antibody conjugates was determined using a Pierce BCA assay kit (Thermo Fisher Scientific). The antibody solutions were aliquoted and stored at 4 °C until use.

Preparation of biological samples

CNS-originating extracellular vesicles (EVs) were isolated from the serum of HC, patients with PD, and patients with MSA as described previously [19]. For analysis of pS^{129}-α-syn in the CSF

of deceased patients with different synucleinopathies and healthy controls, as well as in CNS-originating EVs isolated from human serum, 15 µg total protein, determined using a BCA assay, in 25 µL of Diluent 49 (MSD) were analyzed. Saliva samples obtained from healthy volunteers were centrifuged briefly at 10,000 *g* for 10 min at 4 °C, the clear supernates were collected, and a final volume of 25 µL was used for analysis. Twenty-five µL of clear pooled human serum or plasma containing 1X Halt™ Protease and Phosphatase Inhibitor Cocktail were loaded directly onto the wells. MSA or wild-type mouse brain lysates (5 µg total protein) were diluted in 25 µL Diluent 49 for ECLIA analysis.

ECLIA

The assay was developed using MSD gold 96-well small-spot streptavidin SECTOR ELISA plates. Capture and detection antibody concentrations were determined based on the information available on MSD's website for validation of the human α-synuclein assay. We found that a concentration of 2 µg/mL antibody was sufficient for the capture antibody to saturate the wells of the streptavidin-coated plates (Table S5). Biotinylated-antibody stock solutions were diluted in 1% (w/v) biotin-free bovine serum albumin (bf-BSA) in TBS containing 0.1% (v/v) Tween-20 (TBS-T) to reach a concentration of 2 µg/mL EP1536Y, MJRF1, or MSD's 1X anti-α-syn capture antibody. Dilutions of the semi-synthetic pS^{129}-α-syn, recombinant human α-syn standards, and biological samples were made in Diluent 49 (MSD), which also was used as a "zero" calibrator (blank). One hundred fifty microliters of 3 % (w/v) bf-BSA in TBS-T were added to each well and the plates were incubated with shaking at 800 rpm at RT for 1 h. The blocking solution then was removed and 25 µL of 2 µg/mL or 1X biotinylated capture antibodies were added to each well. The plates were incubated with shaking at 800 rpm at RT for 1 h and then washed three times with 150 µL TBS-T per well. Subsequently, 25 µL of SULFO-TAG detection antibody and

25 µL of samples or standards were added to the wells and the plates were incubated further with shaking at 800 rpm at RT for 2 h. After washing three times with 150 µL TBS-T per well, 150 µL of 1X read buffer (MSD) were added to each well and the plates were read immediately using a Sector S600 reader (MSD). The data were analyzed using Discovery Workbench 4.0 software (MSD) and quantified with reference to freshly prepared standard curves.

Spike recovery

To test spike recovery, a human CSF (DLB) sample, polled serum, a PLP-α-syn mouse brain lysate, or Diluent 49 as a control, were spiked with 250 pg/mL (low spike), 500 pg/mL (medium spike) or 1,000 pg/mL (high spike) of the semi-synthetic pS^{129}-α-syn standard. Twenty-five µL of each spiked or un-spiked sample were analyzed. The spike recovery rate was calculated as the ratio of the measured and the calculated concentration.

Dilution linearity

To test the dilution linearity, all biological samples were serially diluted 2-folds four times in Diluent 49 (MSD). The final volume of each sample was 25 µL. Final concentrations were measured and compared to the calculated concentrations based on the appropriate dilution factor.

Electrospray ionization-mass spectrometry (ESI-MS)

The standard protein was dissolved at 1 mg/mL in ddH_2O, buffer-exchanged into 20 mM ammonium acetate, pH 6.8, using 10-kDa MWCO Amicon centrifugal filters (Millipore Sigma, Burlington, MA), and diluted to 10 µM in the same buffer. The solution was electrosprayed using pulled nanoESI needles onto a Bruker 15T Solarix Fourier-transform ion cyclotron mass spectrometry system. The capillary voltage was set to 800 V and the temperature to 180 °C. The deflector plate was set to 160 V, the capillary exit to 100 V, the funnel voltage to 90 V, and the

skimmer to 50 V. One hundred scans were collected to obtain the spectrum. The deconvolved spectrum was created using UniDec [20].

SDS-PAGE and staining. 1, 0.5, 0.25, or 0.125 µg of pS^{129}-α-syn and 1 µg of unphosphorylated α-syn were fractionated using Sure PAGE 4-20% gradient Bis-Tris gels (GenScript). Samples were prepared by mixing the protein solution with sample buffer (GenScript) and heated at 95 °C for 10 min. Gels were stained in 0.1% (w/v) Coomassie Brilliant Blue (Thermo Fisher Scientific) in 40% (v/v) methanol and 10% (v/v) acetic acid for 1 h at RT and then de-stained in the same solution excluding Coomassie Brilliant Blue. Silver-staining was performed using the SilverXpress Silver Staining Kit (Invitrogen) following the manufacturer's protocol.

Immunoblotting. Following SDS-PAGE fractionation, the proteins were transferred onto polyvinyl difluoride (PVDF) membranes (Thermo Fisher Scientific) for 1 h at 25 V on ice using XCell II Blot Modules (Invitrogen). The membranes were blocked using 5% (w/v) non-fat dry milk in TBS-T (blocking solution) for 1 hour at RT and then incubated with either MJFR1 or EP1536Y at a 1:1,000 dilution in blocking solution overnight at 4 °C with gentle agitation. The membranes then were washed in TBS-T thrice and incubated with HRP-conjugated goat anti-rabbit antibody (Thermo Fisher Scientific) at 1:10,000 dilution in blocking solution for 1 h at RT, developed using SuperSignal West Pico PLUS Chemiluminescent Substrate (Life Technologies), and visualized using an Azure Biosystems c300 Gel Imager.

Turbidity Assay. Twenty micromolar pS^{129} -α-syn was incubated for 0, 6, 12, or 24 h at 37 °C with agitation at 300 rpm. Two microliters of the protein were diluted in 48 µl of TBS and absorbance at 600 nm was recorded as a measure of turbidity (Ultrospec 2000, Pharmacia Biotech).

Data processing and statistical analysis

The sensitivity and dynamic range of each antibody combination were evaluated by determination of the limit of blank (LoB), lower limit of detection (LLoD), lower limit of quantification (LLoQ), and upper limit of quantification (ULoQ). The applied definitions for the LoB, LLoD, LLoQ, and ULoQ are described in Table 2. Data were processed using MSD Discovery Workbench 4.0 software and Prism 9.4 (GraphPad, USA). Standard curves and sample concentrations were calculated using a four-parameter fit and plotted as the mean ± standard deviation of 4 replicates. The intra-assay coefficient of variation (CV) was calculated between standard concentrations measured on the same plate, whereas inter-assay CV was calculated in three independent experiments using different plates. Signal/background (S/B) and signal/noise (S/N) ratios were calculated as averages of three standard concentration points within the linear range of the assay for each antibody pair. Total percent error (TE %) was calculated as: ((calculated concentration – actual concentration) + 2 SD)/actual concentration) × 100. Relative percent error (RE %) was calculated as ((calculated concentration – actual concentration)/actual concentration) × 100 (see Supporting Information). Standard error for the method of standard addition was calculated according to Bruce and Gill [21] using the formula:

$$\boldsymbol{S_x} = \frac{\boldsymbol{S_y}}{|\boldsymbol{m}|}\sqrt{\frac{\boldsymbol{1}}{\boldsymbol{n}} + \frac{\bar{\boldsymbol{y}}^{\boldsymbol{2}}}{\boldsymbol{m^2}\sum(\boldsymbol{x_i}-\bar{\boldsymbol{x}})^{\boldsymbol{2}}}}$$

Results

Evaluation of capture and detection antibody pairs and cross-reactivity with unphosphorylated α-syn

We chose to use the MSD ECLIA platform for the development of a pS^{129}-α-syn assay as it offers high-sensitivity detection at a relatively affordable price and has become widely used in academic institutions, the biotechnology industry, and pharmaceutical companies. The detection

principle in this method is based on light emission from electrochemiluminescent labels conjugated to the detection antibody upon application of voltage to the printed electrodes on the back of the wells. The analyte is captured by biotinylated antibodies bound to a streptavidin-coated plate surface. Having made this choice, we tested different combinations of capture and detection antibodies for the degree of sensitivity and reproducibility of the measurements. A number of antibodies with variable sensitivity and specificity have been developed for specific recognition of pS^{129}-α-syn, some of which are commercially available [22].

A recent study comparing several such antibodies found that the rabbit monoclonal antibody EP1536Y had the highest sensitivity and specificity for pS^{129}-α-syn [23], consistent with a previous study [24]. Some concerns about cross-reactivity of this antibody have been raised in a bioRxiv manuscript by Arlinghaus et al. [25] but were not reproduced in a recent, thorough characterization of six anti-pS^{129}-α-syn antibodies by Lashuel et al. [22]. Therefore, we decided to use this antibody either for capture or for detection in combination with an antibody that recognizes α-syn regardless of its phosphorylation status. Reports in the literature and our own experience suggested that mAb MJFR1 [26] might be a good candidate for this task. In addition, we tested the anti-human α-synuclein antibody supplied with the commercial ECLIA kit sold by MSD.

We tested three different combinations of capture and detection antibodies (Table 1). In two combinations, EP1536Y was used either as a biotinylated capture antibody paired with Sulfo-tag anti-human α-synuclein (MSD) as the detection antibody or as a sulfonated detection antibody combined with a biotinylated MSD anti-human α-synuclein capture antibody. In the third combination, biotinylated MJFR1 was used for capture, and Sulfo-tag EP1536Y for detection.

The sensitivity and reproducibility of each antibody combination were evaluated based on a standard curve generated using the semi-synthetic pS^{129}-α-syn at concentrations ranging from 0.5 to 66,167 pg/mL. Unphosphorylated α-syn standards were used to evaluate the specificity of the assay for the phosphorylated form. Each antibody combination was evaluated in at least five experiments performed in triplicate for each standard. Representative standard curves are shown in Figure 1. Comparison of the sensitivity of the assays using EP1536Y and the anti-human α-synuclein (MSD) antibodies (Table 1) showed that when the former was used as capture and the latter for detection, the sensitivity was substantially higher (LLoD = 6 pg/mL, LLoQ = 14 pg/mL) than the reciprocal configuration (LLoD = 15 pg/mL, LLoQ = 75 pg/mL).

The two configurations had comparable signal-to-baseline (S/B) and signal-to-noise (S/N) ratios (Table S1). In comparison, when mAb MJFR1 was used for capture and EP1536Y for detection, the sensitivity was even lower – LLoD = 32 pg/mL, LLoQ = 97 pg/mL (Table 1), and the S/B and S/N values also were substantially lower than those of the two first antibody configurations (Table S1). Therefore, we did not test the reciprocal configuration. All three configurations showed excellent specificity for pS^{129}-α-syn relative to its unphosphorylated form (Figure 1). Of note, the most sensitive configuration, using biotin-EP1536Y for capture and MSD's anti-human α-synuclein antibody for detection, also had the best reproducibility compared to the other configurations. The intra- and inter-assay CV values were 3.9% and 7.2%, respectively, for this configuration, which also had the widest dynamic range. Thus, this configuration was chosen for subsequent experiments, in which we sought to demonstrate the utility of the assay for the analysis of biological samples. The calculated concentrations, total error (TE %), and relative error (RE %) for the three antibody configurations in Table 1 are given in Tables 3—5,

respectively. The use of a higher Biotin-EP1536Y capture antibody concentration of 5 µg/mL compared to 2 µg/µL did not affect the ECL signal intensity (Table S5).

Determination of pS^{129}-α-syn levels in biological samples

We determined the concentration of pS^{129}-α-syn in CSF samples from seven healthy control subjects as well as patients with synucleinopathies (3 PD, 2 DLB, 3 MSA). Due to an apparent moderate matrix effect seen in the CSF (see below), the measured values were corrected using the method of standard addition [27].

The pS^{129}-α-syn concentration levels were variable (Figure 2A) and the small sample numbers did not allow meaningful comparison among the groups. In different samples of commercial, pooled, human serum we determined pS^{129}-α-syn levels to be 58 ± 23 pg/mL whereas in human plasma the concentration was 7 ± 3 pg/mL, suggesting that the anticoagulants in the plasma might interfere with the assay. Measurement of pS^{129}-α-syn concentrations in the saliva of two healthy control subjects yielded an average concentration of 15 ± 3 pg/mL (Figure 2A). The concentrations measured in plasma and saliva samples were mostly below the LLoQ and some were below the LLoD. The saliva results likely reflect the fact that samples from healthy people are expected to contain very low levels of pS129-α-syn, whereas those in the plasma suggest a matrix effect as discussed below. We also analyzed brain lysates from wild-type mice and PLP-α-syn mice, a transgenic model of multiple system atrophy in which α-syn is overexpressed under the PLP promoter [18], leading to its accumulation in oligodendrocytes [28].

The concentration of pS^{129}-α-syn in the soluble fraction of mouse brain extracts (5 µg of total protein) from the PLP-α-syn mice was 19,381 ± 13,173 pg/mL, > 50-fold higher than in brain extracts from wild-type mice (433 ± 120 pg/mL, Figure 2B). These findings are in agreement with the known accumulation of the phosphorylated protein in the brains of the MSA-model

mice [29], demonstrating the utility of the assay for mouse experiments. Finally, we isolated neuronal EVs (nEVs) and oligodendroglial EVs (oEVs) from the serum of healthy controls, patients with PD, and patients with MSA, as described previously, and measured the pS^{129}-α-syn levels in these samples. The analysis showed concentrations between 1.5 and 248.9 pg/mL in nEVs and between 2.2 and 379.9 pg/mL in oEVs. When the measurements of pS^{129}-α-syn in the CNS-originating EVs were combined with the previous analysis of total α-syn [19], the separation improved among all the groups [30], demonstrating the importance and utility of the new assay.

Dilution linearity and spike recovery

Next, we tested the dilution linearity and spike recovery in biological samples, different from those used in the previous experiments, including human CSF from a patient with DLB (undiluted concentration 113 ± 14 pg/mL), pooled human serum (undiluted 39 ± 9 pg/mL), and a PLP-α-syn mouse brain lysate (undiluted 14,265 ± 457 pg/mL). Acceptable recovery rates were defined as 100 ± 20%. The experiments showed reasonable linearity in the CSF up to 1:8 (Figure 3A) and in the serum up to 1:4 dilution (Figure 3B), likely reflecting the drop of the concentration at higher dilutions below the LLoQ. The dilution linearity was consistent for the PLP-α-syn mouse brain lysate samples (Figure 3C) thanks to the high concentration of pS^{129}-α-syn in these samples, maintaining the concentration well above the LLoQ at all dilutions.

Spike recovery was tested in the same CSF, serum, and MSA mouse-brain extract samples at three concentrations – 250, 500, and 1,000 pg/mL. These concentrations were chosen to cover the lower end of the dynamic range, in view of the low concentrations we detected in the human samples (Figure 2). The recovery in CSF samples was low, particularly in the samples spiked with low concentrations (Figure 3D) suggesting that CSF components partially interfere with the

signal and therefore the concentrations measured in this medium might be an underrepresentation of the actual pS^{129}-α-syn concentration. To address this issue, as described above, we used the method of standard addition to correct the pS^{129}-α-syn concentrations measured in the CSF. Good recovery was observed in both the serum (Figure 3E) and mouse-brain extract (Figure 3F) samples.

Evaluation of pS^{129}-α-syn standard stability

During the course of the work described above, we observed on multiple occasions deterioration of the signal of the pS^{129}-α-syn standard within 1–2 weeks of storage, prompting a detailed investigation to identify the possible causes of this issue and potential solutions. We compared reconstitution of the protein in ddH_2O or TBS, pH 7.4, with or without pre-treatment with trifluoroacetic acid (TFA), filtered through 10- or 100-kDa MWCO filters to remove pre-formed aggregates, and used 1.0 mg/mL or lower concentrations of the standard protein for the stock solution. In all cases, the solution was aliquoted into single-use aliquots and stored at -80 °C until it was used in the assay. When this solution was used immediately after preparation, the ECLIA signal for the highest-concentration standard, 100 ng/mL, was between 4×10^5 and 1.1×10^6. This level of variability is similar to that reported by MSD for their total α-syn ECLIA kits. However, on multiple occasions, within 1–2 weeks of preparing the stock solution, the signal for this standard deteriorated by 10-20-fold, raising concern that the dynamic range of the assay would be too low for meaningful measurement and comparison among experiments would become difficult.

In view of the observed signal deterioration during the storage of the diluted and aliquoted protein standard, we tested whether it might have lost the phosphate group on Ser^{129}. Examination of the protein by ESI-MS revealed that it had the intact mass with the expected

phosphorylation (Figure 4), ruling out this option. Thus, we hypothesized next that the loss of signal could be due to oligomerization or aggregation of the protein during the preparation process, creating seeds that would promote further rapid aggregation, even when the protein is stored at -80 °C. Indeed, under most of the conditions we used, we observed high-molecular-weight bands of pS^{129}-α-syn using SDS-PAGE fractionation followed by Coomassie Blue staining (Figure 5A), silver-staining (Figure 5B), or western-blots probed with antibodies MJFR1 (Figure 5C) or EP1536Y (Figure 5D). Unphosphorylated α-syn was used as a control in these experiments and migrated as a monomer only (Figure 5A–C). Changing the solution from ddH_2O to TBS and filtering the stock solution did not resolve the issue. Reducing the concentration of the stock solution to 0.29 mg/mL, as recommended by Cariulo et al. [12] reduced the aggregation but the signal loss was still observed if the TFA used for the initial dissolution of the protein powder was not removed completely.

EP1536Y has been used in immunohistochemistry studies to detect aggregated pS129-α-syn in LBs or GCIs [23]. Therefore, the interpretation of the signal loss in the ELICA assay as reflecting aggregation was counterintuitive. To further examine this idea, we incubated the protein with agitation for up to 24 h, monitored occasionally its aggregation using a turbidity assay, and measured the signal of the highest standard (100 ng/mL) at the same time points (Figure 5E). These experiments revealed that the protein indeed aggregated concomitant with a substantial decrease in the ECLIA signal.

Following the protocol published by Cariulo et al. [12] precisely and ensuring that the TFA was removed completely, was necessary for preventing seed formation and allowing the protein to remain unaggregated for prolonged storage. Under these conditions, weekly repeated testing of the standard curve and positive control samples (MSA mouse-brain extract) yielded consistent

data over one month without apparent signal loss. Analysis of the protein prepared in this manner using SDS-PAGE followed by Coomassie Blue staining (Figure 6A), silver-staining (Figure 6B), or western blots probed with MJFR1 (Figure 6C) or EP1536Y (Figure 6D) showed an absence of the previously observed high-molecular-weight bands.

Discussion

High throughput measurement of disease-relevant, post-translationally modified forms of α-syn with high sensitivity currently is an unmet need for clinical and biomarker studies. To address this need, we developed a novel assay based on the MSD ECLIA platform that detects and quantifies pS^{129}-α-syn at low pg/mL concentrations in various biological samples. The assay does not detect unphosphorylated forms of α-syn up to concentrations >10 ng/mL (Figure 1). The specificity and high sensitivity of the assay are achieved thanks to the use of monoclonal antibody EP1536Y for the capture of the analyte followed by detection by the Sulfo-Tag anti-α-syn antibody provided in MSD's total α-syn kit. Compared to the two other antibody combinations/configurations we attempted, this capture and detection combination provided not only the highest sensitivity but also the highest dynamic linear range and best reproducibility. In agreement with this finding, other groups showed that the EP1536Y antibody is highly specific for pS^{129}-α-syn and could detect it robustly even in the presence of other post-translational modifications in close proximity to Ser^{129} compared to other evaluated anti-pS^{129}-α-syn antibodies [15, 22-24].

However, interference of other post-translational modifications and phosphorylation at other sites of α-syn were not assessed in our assay. Lashuel and colleagues reported that EP1536Y does detect α-syn phosphorylated at both Tyr125 and Ser129 and does not detect pS^{129}-α-syn truncated after residues 133 or 135. In addition, the antibody showed a reduced signal when tested for

binding of α-syn fibrils phosphorylated at Ser129 and nitrated at Tyr125, Tyr133, and Tyr136 compared to fibrils of pS^{129}-α-syn itself [22]. The contribution of these other post-translationally modified α-syn forms to the signal in the biological samples we tested here or to the levels of pS^{129}-α-syn measured in previous studies currently is not known.

When comparing the ECLIA platform described here with other published methods for quantifying pS^{129}-α-syn in biological fluids, it is important to note the lack of consensus in the data from different groups. For example, Wang et al. reported pS^{129}-α-syn concentrations of 58–80 pg/mL in the CSF of patients with PD or MSA using a bead-based Luminex assay [10], whereas Majbour et al. found substantially higher pS^{129}-α-syn concentration levels, 181–275 pg/mL in the CSF of healthy individuals and 207–296 pg/mL in the CSF of patients with PD determined by a sandwich ELISA [11]. These assays used casein kinase II to phosphorylate recombinant α-syn, which was used as a standard, and Wang et al. diluted their samples by ¾, whereas Majbour et al. did not. The corrected pS^{129}-α-syn concentrations we detected in CSF samples were between 32–191 pg/mL (Figure 2), in rough agreement with both studies.

In contrast, a study by Cariulo et al. did not detect pS^{129} α-syn in pooled commercial CSF despite using a highly sensitive Singulex Erenna immunoassay with a LLoD of 0.15 pg/mL [12]. This apparent discrepancy may be explained in part by the differences between the particle-based digital single-molecule counting in the Singulex Erenna and the electrochemiluminescence signal measured by ECLIA, which allowed us to use a different sample preparation process that did not require transfer of beads multiple times to different tubes/plates, followed by the appropriate wash steps, which might have helped reduce the loss of signal by non-specific adsorption to surfaces. In addition, the antibody we used, EP1536Y, has been reported by to have higher sensitivity and specificity compared to the one used by Cariulo et al. MJF-R13 (8-8) [23],

presumably increasing further our ability to detect pS129-α-syn in the CSF. In contrast, using IP-MS/MS, Lashuel and co-workers also did not detect pS^{129} α-syn in the CSF of patients with PD and healthy controls, highlighting the difficulty and inconsistency in measuring this α-syn species in CSF [23].

To our knowledge, one previous study tested pS^{129}-α-syn in serum using a modified paired-surface plasma-wave biosensor and reported concentrations in the range 500 to 5,000 pg/mL in HC and 4,000 to 12,000 pg/mL in patients with PD [31]. The large differences between the technique used in that paper and the ECLIA used here make comparison with our data difficult. Our data suggest that plasma components may interfere with the assay (Figure 2). The plasma signal in our assay was an order of magnitude lower than the signal observed in serum samples. The two fluids differ mainly by the presence of anticoagulants in plasma, and possibly coagulation factors, e.g., fibrinogen, which may interfere with the assay. As both types of samples were commercial, pooled biofluids and not taken from the same persons, a direct comparison was not possible. Previous studies by Foulds et al. in two separate cohorts found 200–600 ng/mL [6] and 143 ± 532 ng/mL pS^{129}-α-syn [14] in control human plasma, several orders of magnitude above the concentrations we measured. However, these results also were over three orders of magnitude higher than the concentrations we found in serum, suggesting that assay differences likely were the main reason for these large discrepancies. In the study by Cariulo et al., pS^{129} α-syn levels in the range 480 – 1223 pg/mL were found for clinically obtained and commercially pooled plasma samples [12]. The large discrepancy in values may be attributed to the differences in the assays themselves, batch variation, sample source, sample processing, and the antibody pairs used, as discussed above.

The MSD ECLIA platform used for this assay is a highly sensitive, versatile, and widespread technology, and similar to the other platforms, allows duplexing of assays, for example for quantification of pS^{129} α-syn and unphosphorylated α-syn together. Creating such a duplex assay is outside the scope of the current work but we expect to develop it in the future. Notwithstanding the limitations discussed above, our results suggest that the pS^{129}-α-syn ECLIA is an attractive tool for measuring pS^{129}-α-syn in CSF, serum, saliva, potentially other biofluids, brain lysates, or other experimental systems, such as cell cultures and animal models. Nevertheless, cross-validation of our assay by other groups, thorough validation of the used antibodies, and strictly standardized sample preparation protocols are crucial for achieving reliable and reproducible results. We anticipate that future commercial kits will provide small aliquots of the standard that can be prepared freshly for single use. Until such assays become available, researchers interested in using the assay are advised to follow carefully the protocol published by Cariulo et al. [12] to ensure that the semi-synthetic pS^{129}-α-syn, which currently is sold by Proteos only in 1-mg portions, is not lost due to aggregation shortly after its preparation.

FIGURES

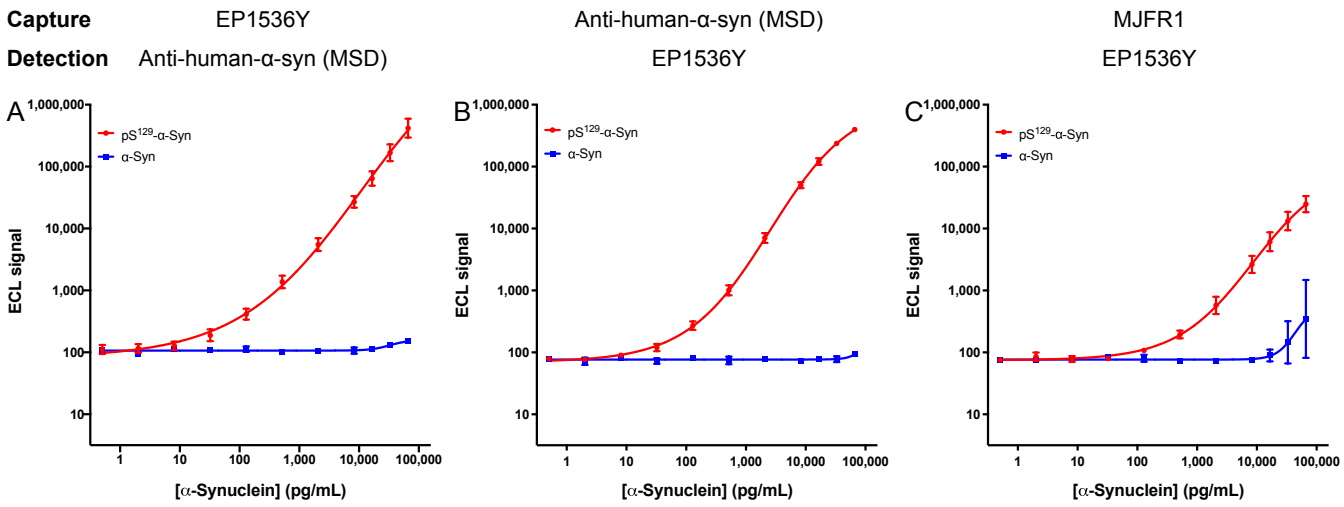

Figure 1. Standard curves for pS^{129}-α-syn (red) and unphosphorylated α-syn standards (blue) using different antibody configurations. A) Biotinylated EP1536Y used for capture and Sulfo-tagged MSD's anti-human-α-synuclein antibody for detection. B) Biotinylated MSD's anti-human-α-synuclein antibody used for capture and Sulfo-tagged EP1536Y for detection. C) Biotinylated mAb MJFR1 was used for capture and Sulfo-tagged EP1536Y for detection. Representative standard curves (Mean ± SD of two technical replicates) of at least five independent experiments are shown.

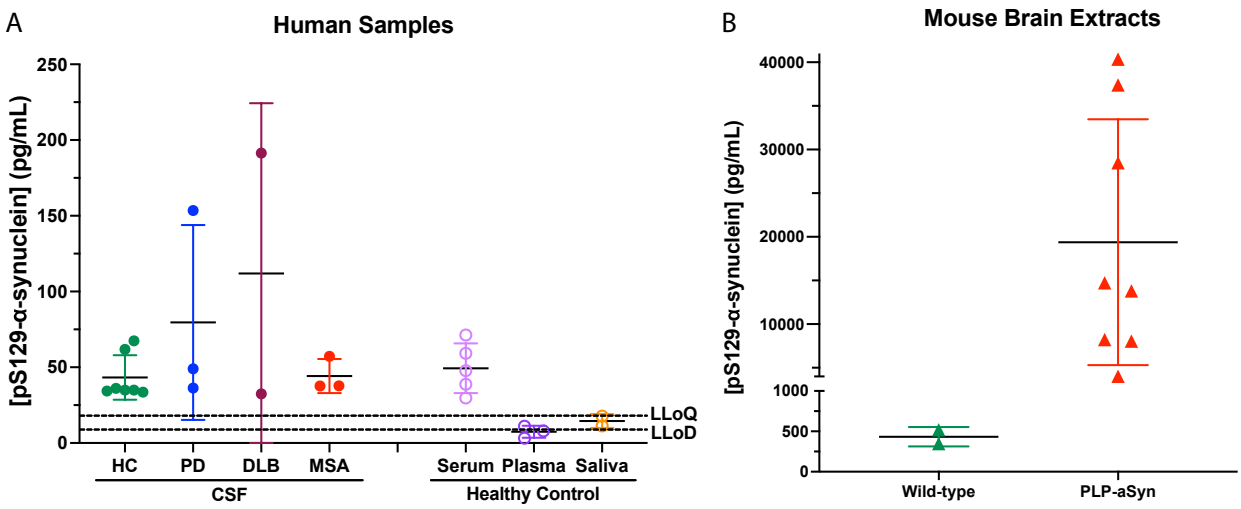

Figure 2. Measurement of pS^{129} α-syn in human and mouse samples. All measurements were performed using biotinylated EP1536Y for capture and MSD's Sulfo-tagged anti-human-α-synuclein antibody for detection. A) Measurement of pS^{129}-α-syn in human CSF, serum, plasma, and saliva. HC – healthy control, PD – Parkinson's disease, DLB – dementia with Lewy bodies, MSA – multiple system atrophy, LLoD – lower limit of detection, LLoQ – lower limit of quantitation. B) Comparison of pS^{129} α-syn concentrations in brain extracts from wild-type and MSA model mice. The data are shown as mean ± SD.

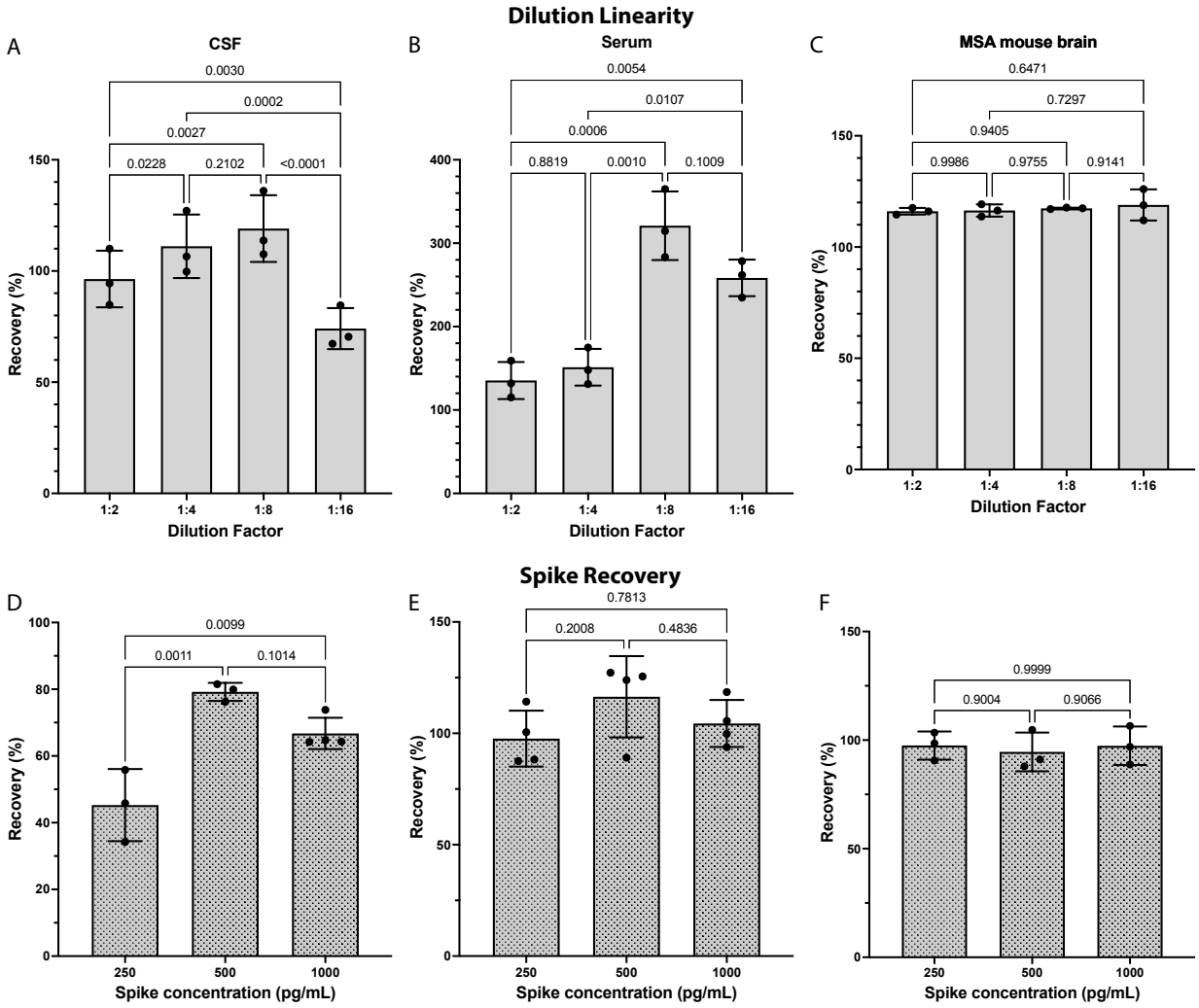

Figure 3. Dilution linearity and spike recovery. A-C) Dilution linearity within a 2-fold dilution series in A) human CSF from a patient with DLB, B) pooled human serum, and C) extracts of PLP-α-syn mouse brain. The experiments were analyzed by repeated-measure one-way ANOVA with Tukey's multiple comparisons test with a single pooled variance. D-F) Spike recovery rates after the addition of 250, 500, or 1000 pg/mL semi-synthetic pS^{129}-α-syn to D) human CSF from a patient with DLB, E) pooled human serum, and F) extracts of PLP-α-syn mouse brain. The experiments were analyzed by ordinary one-way ANOVA with Tukey's multiple comparisons test with a single pooled variance. The data are shown as mean ± SD.

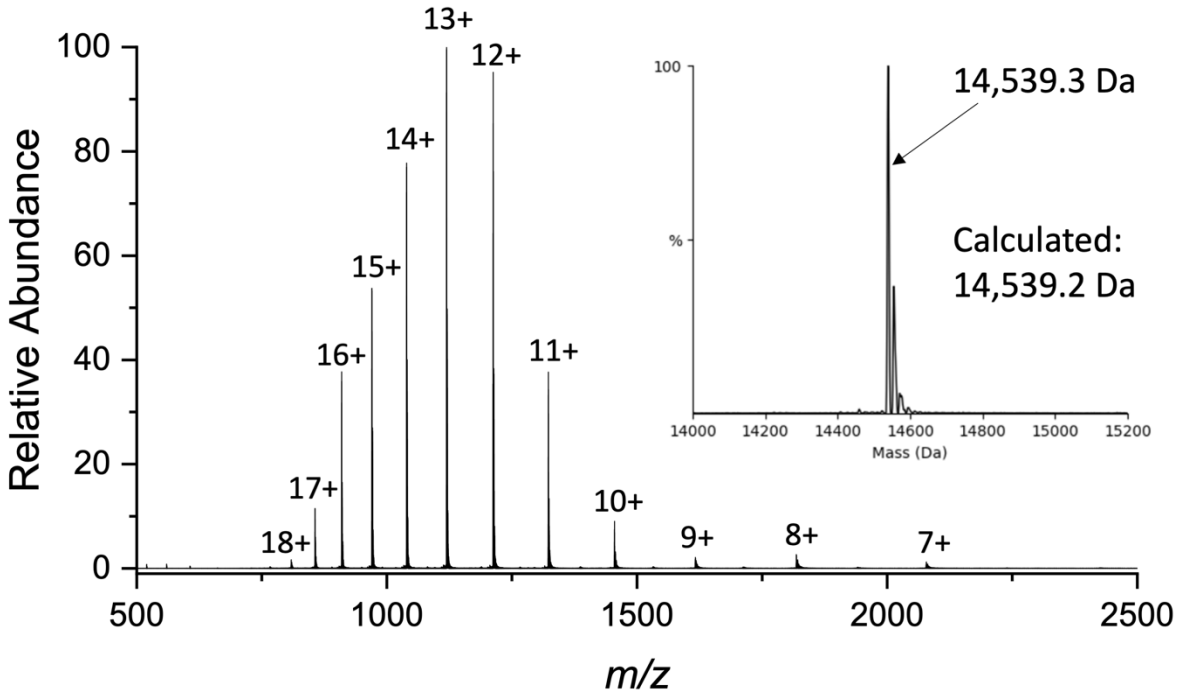

Figure 4. Mass spectrometry analysis of the pS^{129} α-syn standard. An ESI mass-spectrum of pS^{129}-α-syn. The inset shows the deconvoluted spectrum corresponding to a single protein species with the correct mass of pS^{129}-α-syn.

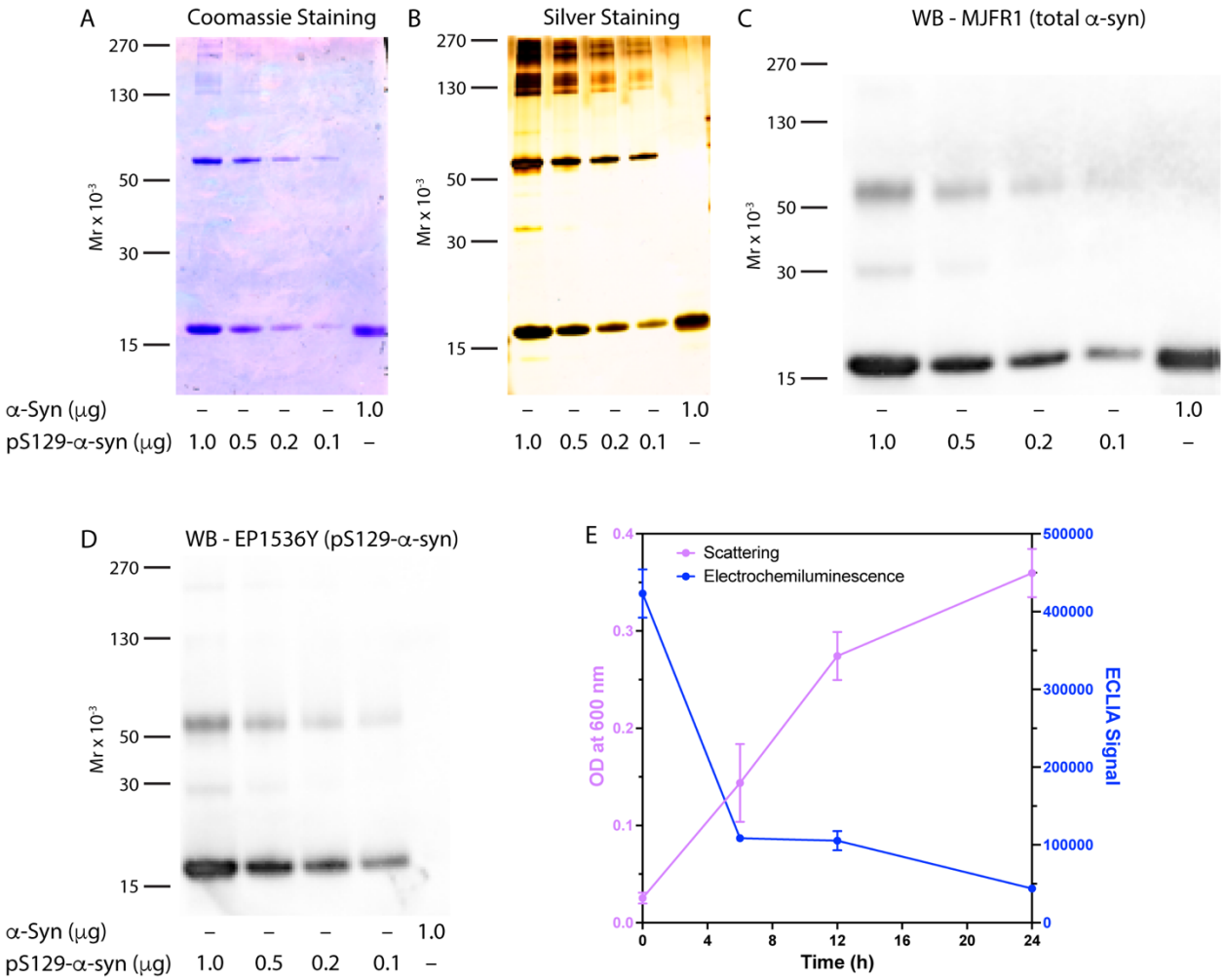

Figure 5. The pS[129]-α-syn standard aggregates when prepared using non-optimized conditions. A-D) Different quantities of the semi-synthetic pS[129]-α-syn standard were fractionated and unphosphorylated α-syn was used as a control. A) Coomassie Blue staining shows the presence of oligomers, presumably tetramers, and larger aggregates of pS[129]-α-syn but not of unphosphorylated α-syn. B) Higher-sensitivity visualization of the same gel by silver staining. C) Western blot analysis probed with the anti-α-syn antibody MJFR1. D) Western blot analysis probed with the anti-pS[129]-α-syn antibody EP1536Y. The gel migration of molecular weight markers is shown on the left in each panel. E) 100 ng/mL pS[129]-α-syn were incubated at 37 °C for the indicated times, at which turbidity was measured as absorbance (scattering) at 600 nM and the electrochemiluminescence signal was measured as described in the Methods section.

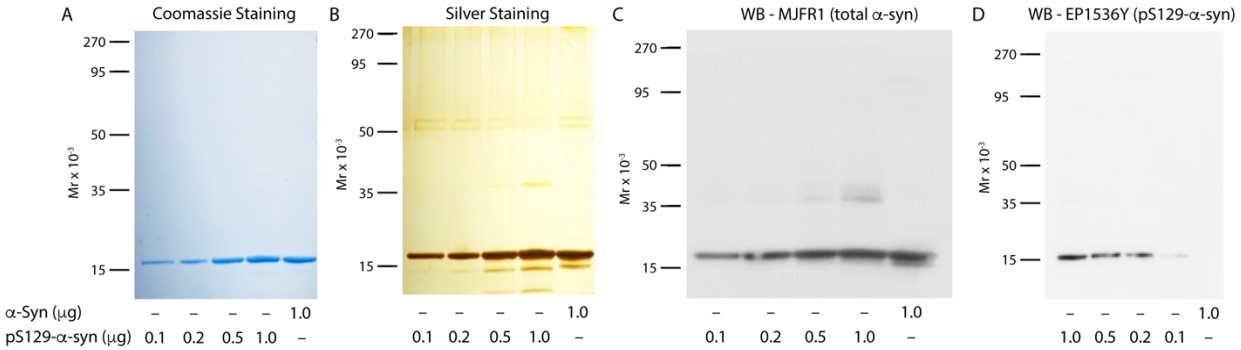

Figure 6. SDS-PAGE and western-blot analysis of the pS^{129}-α-syn standard prepared using optimized conditions. Different quantities of the semi-synthetic pS^{129}-α-syn standard were fractionated and unphosphorylated α-syn was used as a control. A) Coomassie Blue staining shows an absence of oligomers of pS^{129} α-syn. B) Higher-sensitivity visualization of the same gel by silver staining shows minor bands of a putative dimer in the 0.5- and 1.0-μg pS^{129}-α-syn lanes. Minor degradation products are also observed under the monomer band. Bands between 50–60 kDa likely are keratin contamination and are not related to the analyzed proteins. C) Western blot analysis probed with the anti-α-syn antibody MJFR1 showing minor putative dimer bands in the 0.5- and 1.0-μg pS^{129}-α-syn lanes. D) Western blot analysis probed with the anti-pS^{129}-α-syn antibody EP1536Y. The gel migration of molecular weight markers is shown on the left in each panel.

Table 1: Evaluation of antibody combinations for development of the pS^{129}-α-synuclein electrochemiluminescence ELISA.

Capture antibody	Detection antibody	LoB (pg/mL)	LLoD (pg/mL)	LLoQ (pg/mL)	ULoQ (pg/mL)	Intra-assay CV (%)	Inter-assay CV (%)
Biotin-EP1536Y (anti-pS^{129}-α-syn)	Anti-human α-syn-Sulfo tag (MSD)	3.1 ± 0.6	6 ± 3	14 ± 10	66,167	3.9	7.2
Biotin-anti-human α-syn (MSD)	EP1536Y-Sulfo tag	11 ± 3	15 ± 8	75 ± 13	33,088	4.6	10.5
Biotin-MJFR1 (anti-human α-syn)	EP1536Y-Sulfo tag	11 ± 10	32 ± 10	97 ± 30	33,088	7.2	28.3

Mean ± SD are shown for LoB, LLoD, and LLoQ.

Table 2: Definitions of assay parameters [32].

LoB	Calculated concentration based on the mean zero calibrator signal + 1.645 × the standard deviation (SD) of the zero calibrators.
LLoD	Calculated concentration based on the signal + 1.645 × SD (lowest calibrator) above the LoB.
LLoQ	Calculated concentration based on the signal + 10 × SD (blank) above the zero calibrators.
ULoQ	Calibrator concentration at the upper limit of the linear range on a logarithmic scale.

Table 3: Signal/background (S/B) and signal/noise (S/N) ratios for pS^{129} α-syn and α-syn of the evaluated antibody pairs [33].

Capture antibody	Detection antibody	S/B (pS^{129} α-syn)	S/N (pS^{129} α-syn)	S/B (α-syn)	S/N (α-syn)
Biotin-EP1536Y (anti-pS^{129}-α-syn)	Anti-human α-syn-Sulfo tag (MSD)	426	43674	1	86
Biotin-anti-human α-syn (MSD)	EP1536Y-Sulfo tag	651	49217	1	65
Biotin-MJFR1 (anti-human α-syn)	EP1536Y-Sulfo tag	37	2791	1	43

The S/B and S/N ratios are averages of three standard concentration points within the linear range of the assay using each antibody pair.

Table 4: Calculated concentrations, total error (TE) [33] and relative error (RE) [34] of pS^{129}-α-syn ECLIA using EP1536Y for capture and anti-human α-syn antibody (MSD) for detection.

pS^{129}-α-syn (pg/mL)	Assay 1		Assay 2		Assay 3	TE (%)	RE (%)
	1	2	1	2	1		
66176	77102	65766	68279	71620	66202	18.4	5.7
33088	33119	31361	32100	33769	34979	10.9	3.2
16544	14916	15799	14657	16233	15718	13.6	6.5
8272	7836	8250	7690	7918	8151	8.6	3.7
2068	2269	2148	2266	2244	2004	16.7	7.0
517	613	571	604	605	550	23.2	13.8
129	126	124	122	122	141	16.4	5.3
32	18	23	26	21	32	54.8	25.0
8	5.7	4.4	3.8	4.7	5.9	58.6	38.8
2	1.7	4.0	2.1	2.5	0.8	146.3	41.0
0.5	1.5	2.2	2.1	1.8	1.7	375.1	272.0

TE (%) = ((calculated concentration – actual concentration) + 2 SD)/actual concentration) × 100;

RE (%) = ((calculated concentration – actual concentration)/actual concentration) × 100.

Table 5: Calculated concentrations, total error (TE) [33] and relative error (RE) [34] of pS^{129}-α-syn ECLIA using the Biotin-MJFR1 - EP1536Y-Sulfo tag antibody pair.

pS^{129} α-syn (pg/mL)	Assay 1		Assay 2		TE (%)	RE (%)
	1	2	1	2		
66176	60951	65118	64829	69720	13.6	4.2
33088	33826	34340	32593	34348	7.2	2.8
16544	16393	18542	15645	17102	18.4	5.4
8272	9349	7820	7639	8187	22.9	6.8
2068	1631	1791	2338	2130	39.5	12.6
517	397	298	470	585	62.6	22.0
129	468	751	108	97	618.6	196.4
32	7.0	n.d.	15	10	86.8	66.7
8	2.0	n.d.	8.2	28	384.4	108.5
2	39	10	n.d.	17	2198.9	999.1
0.5	0.6	n.d.	2.9	2.9	752.1	317.5

n.d. – not determined

Table 6: ECL signal of pS^{129} α-syn standards using 2 or 5 µg/mL Biotin-EP1536Y capture antibody and MSD Sulfo-tag antibody for detection.

pS^{129} α-syn (pg/mL)	2 µg/mL capture antibody	5 µg/mL capture antibody
10000	107291	103256
2500	17083	16278
625	3529	3507
156	957	902
39	332	317
9.8	152	135
2.4	116	95
0	96	91

References

[1] Spillantini MG, Crowther RA, Jakes R, Hasegawa M, Goedert M (1998) alpha-Synuclein in filamentous inclusions of Lewy bodies from Parkinson's disease and dementia with lewy bodies. *Proc Natl Acad Sci U S A* **95**, 6469-6473.

[2] Spillantini MG, Schmidt ML, Lee VM, Trojanowski JQ, Jakes R, Goedert M (1997) Alpha-synuclein in Lewy bodies. *Nature* **388**, 839-840.

[3] Marti MJ, Tolosa E, Campdelacreu J (2003) Clinical overview of the synucleinopathies. *Mov Disord* **18 Suppl 6**, S21-27.

[4] Anderson JP, Walker DE, Goldstein JM, de Laat R, Banducci K, Caccavello RJ, Barbour R, Huang J, Kling K, Lee M, Diep L, Keim PS, Shen X, Chataway T, Schlossmacher MG, Seubert P, Schenk D, Sinha S, Gai WP, Chilcote TJ (2006) Phosphorylation of Ser-129 is the dominant pathological modification of α-synuclein in familial and sporadic Lewy body disease. *Journal of Biological Chemistry* **281**, 29739-29752.

[5] Fujiwara H, Hasegawa M, Dohmae N, Kawashima A, Masliah E, Goldberg MS, Shen J, Takio K, Iwatsubo T (2002) alpha-Synuclein is phosphorylated in synucleinopathy lesions. *Nat Cell Biol* **4**, 160-164.

[6] Foulds PG, Mitchell JD, Parker A, Turner R, Green G, Diggle P, Hasegawa M, Taylor M, Mann D, Allsop D (2011) Phosphorylated α-synuclein can be detected in blood plasma and is potentially a useful biomarker for Parkinson's disease. *FASEB Journal* **25**, 4127-4137.

[7] Majbour NK, Vaikath NN, Eusebi P, Chiasserini D, Ardah M, Varghese S, Haque ME, Tokuda T, Auinger P, Calabresi P, Parnetti L, El-Agnaf OM (2016) Longitudinal changes

in CSF alpha-synuclein species reflect Parkinson's disease progression. *Mov Disord* **31**, 1535-1542.

[8] MyBioSource, Human Phosphorylated Alpha Synuclein ELISA Kit, https://www.mybiosource.com/psnca-human-elisa-kits/phosphorylated-alpha-synuclein/38716, Accessed 06. Oct. 2022.

[9] Schulz I, Kruse N, Gera RG, Kremer T, Cedarbaum J, Barbour R, Zago W, Schade S, Otte B, Bartl M, Hutten SJ, Trenkwalder C, Mollenhauer B (2021) Systematic Assessment of 10 Biomarker Candidates Focusing on α-Synuclein-Related Disorders. *Movement Disorders* **36**, 2874-2887.

[10] Wang Y, Shi M, Chung KA, Zabetian CP, Leverenz JB, Berg D, Srulijes K, Trojanowski JQ, Lee VM, Siderowf AD, Hurtig H, Litvan I, Schiess MC, Peskind ER, Masuda M, Hasegawa M, Lin X, Pan C, Galasko D, Goldstein DS, Jensen PH, Yang H, Cain KC, Zhang J (2012) Phosphorylated α-synuclein in Parkinson's disease. *Science Translational Medicine* **4**, 121ra120.

[11] Majbour NK, Vaikath NN, van Dijk KD, Ardah MT, Varghese S, Vesterager LB, Montezinho LP, Poole S, Safieh-Garabedian B, Tokuda T, Teunissen CE, Berendse HW, van de Berg WD, El-Agnaf OM (2016) Oligomeric and phosphorylated α-synuclein as potential CSF biomarkers for Parkinson's disease. *Molecular Neurodegeneration* **11**, 7.

[12] Cariulo C, Martufi P, Verani M, Azzollini L, Bruni G, Weiss A, Deguire SM, Lashuel HA, Scaricamazza E, Sancesario GM, Schirinzi T, Mercuri NB, Sancesario G, Caricasole A, Petricca L (2019) Phospho-S129 α-Synuclein Is Present in Human Plasma but Not in Cerebrospinal Fluid as Determined by an Ultrasensitive Immunoassay. *Frontiers in Neuroscience* **13**, 889.

[13] Landeck N, Hall H, Ardah MT, Majbour NK, El-Agnaf OM, Halliday G, Kirik D (2016) A novel multiplex assay for simultaneous quantification of total and S129 phosphorylated human α-synuclein. *Molecular Neurodegeneration* **11**, 61.

[14] Foulds PG, Diggle P, Mitchell JD, Parker A, Hasegawa M, Masuda-Suzukake M, Mann DM, Allsop D (2013) A longitudinal study on α-synuclein in blood plasma as a biomarker for Parkinson's disease. *Scientific Reports* **3**, 2540.

[15] Tian C, Liu G, Gao L, Soltys D, Pan C, Stewart T, Shi M, Xie Z, Liu N, Feng T, Zhang J (2019) Erythrocytic α-Synuclein as a potential biomarker for Parkinson's disease. *Translational Neurodegeneration* **8**, 15.

[16] Waxman EA, Giasson BI (2008) Specificity and regulation of casein kinase-mediated phosphorylation of alpha-synuclein. *J Neuropathol Exp Neurol* **67**, 402-416.

[17] Fauvet B, Lashuel HA (2016) Semisynthesis and Enzymatic Preparation of Post-translationally Modified alpha-Synuclein. *Methods Mol Biol* **1345**, 3-20.

[18] Herrera-Vaquero M, Bouquio D, Kallab M, Biggs K, Nair G, Ochoa J, Heras-Garvin A, Heid C, Hadrovic I, Poewe W, Wenning GK, Klärner FG, Schrader T, Bitan G, Stefanova N (2019) The molecular tweezer CLR01 reduces aggregated, pathologic, and seeding-competent α-synuclein in experimental multiple system atrophy. *Biochimica et Biophysica Acta - Molecular Basis of Disease* **1865**, 165513.

[19] Dutta S, Hornung S, Kruayatidee A, Maina KN, Del Rosario I, Paul KC, Wong DY, Duarte Folle A, Markovic D, Palma JA, Serrano GE, Adler CH, Perlman SL, Poon WW, Kang UJ, Alcalay RN, Sklerov M, Gylys KH, Kaufmann H, Fogel BL, Bronstein JM, Ritz B, Bitan G (2021) α-Synuclein in blood exosomes immunoprecipitated using

neuronal and oligodendroglial markers distinguishes Parkinson's disease from multiple system atrophy. *Acta Neuropathol* **142**, 495-511.

[20] Marty MT, Baldwin AJ, Marklund EG, Hochberg GK, Benesch JL, Robinson CV (2015) Bayesian deconvolution of mass and ion mobility spectra: from binary interactions to polydisperse ensembles. *Analytical Chemistry* **87**, 4370-4376.

[21] Bruce GR, Gill PS (1999) Estimates of Precision in a Standard Additions Analysis. *Journal of Chemical Education* **76**, 805.

[22] Lashuel HA, Mahul-Mellier AL, Novello S, Hegde RN, Jasiqi Y, Altay MF, Donzelli S, DeGuire SM, Burai R, Magalhaes P, Chiki A, Ricci J, Boussouf M, Sadek A, Stoops E, Iseli C, Guex N (2022) Revisiting the specificity and ability of phospho-S129 antibodies to capture alpha-synuclein biochemical and pathological diversity. *NPJ Parkinsons Dis* **8**, 136.

[23] Delic V, Chandra S, Abdelmotilib H, Maltbie T, Wang S, Kem D, Scott HJ, Underwood RN, Liu Z, Volpicelli-Daley LA, West AB (2018) Sensitivity and specificity of phospho-Ser129 α-synuclein monoclonal antibodies. *The Journal of Comparative Neurology* **526**, 1978-1990.

[24] Rutherford NJ, Brooks M, Giasson BI (2016) Novel antibodies to phosphorylated α-synuclein serine 129 and NFL serine 473 demonstrate the close molecular homology of these epitopes. *Acta Neuropathologica Communications* **4**, 80.

[25] Arlinghaus R, Iba M, Masliah E, Cookson MR, Landeck N (2023) Specific Detection of Physiological S129 Phosphorylated alpha-Synuclein in Tissue Using Proximity Ligation Assay. *J Parkinsons Dis* **13**, 255-270.

[26] Gray MT, Munoz DG, Gray DA, Schlossmacher MG, Woulfe JM (2014) α-Synuclein in the appendiceal mucosa of neurologically intact subjects. *Movement Disorders* **29**, 991-998.

[27] Bader M (1980) A systematic approach to standard addition methods in instrumental analysis. *Journal of Chemical Education* **57**, 703.

[28] Refolo V, Bez F, Polissidis A, Kuzdas-Wood D, Sturm E, Kamaratou M, Poewe W, Stefanis L, Angela Cenci M, Romero-Ramos M, Wenning GK, Stefanova N (2018) Progressive striatonigral degeneration in a transgenic mouse model of multiple system atrophy: translational implications for interventional therapies. *Acta Neuropathologica Communications* **6**, 2.

[29] Stefanova N, Wenning GK (2015) Animal models of multiple system atrophy. *Clinical Autonomic Research* **25**, 9-17.

[30] Taha HB, Hornung S, Dutta S, Fenwick L, Lahgui O, Howe K, Elabed N, Del Rosario I, Wong DY, Duarte Folle A, Markovic D, Palma JA, Kang UJ, Alcalay RN, Sklerov M, Kaufmann H, Fogel BL, Bronstein JM, Ritz B, Bitan G (2023) Toward a biomarker panel measured in CNS-originating extracellular vesicles for improved differential diagnosis of Parkinson's disease and multiple system atrophy. *Transl Neurodegener* **12**, 14.

[31] Chen WR, Chen JC, Chang SY, Chao CT, Wu YR, Chen CM, Chou C (2021) Phosphorylated α-synuclein in diluted human serum as a biomarker for Parkinson's disease. *Biomedical Journal*.

[32] Armbruster DA, Pry T (2008) Limit of blank, limit of detection and limit of quantitation. *The Clinical Biochemist Reviews* **29 Suppl 1**, S49-52.

[33] Westgard JO, Carey RN, Wold S (1974) Criteria for judging precision and accuracy in method development and evaluation. *Clinical chemistry* **20**, 825-833.

[34] Kat C-J, Els PS (2012) Validation metric based on relative error. *Mathematical and Computer Modelling of Dynamical Systems* **18**, 487-520.

Chapter 2

Toward a Biomarker Panel measured in CNS-originating Extracellular Vesicles for Improved Differential Diagnosis of Parkinson's Disease and Multiple System Atrophy

Edited & Expanded Version.

Translational Neurodegeneration

Publication Date: March 20th, 2023

https://doi.org/10.1186/s40035-023-00346-0

ABSTRACT

Background: Current antemortem differential diagnosis of Parkinson's disease (PD) and multiple system atrophy (MSA) is challenging due to the overlap of parkinsonian symptoms, especially in the early stages of disease. Analysis of biomarkers in CNS-originating extracellular vesicles (EVs) isolated from blood is a promising strategy for these diseases. EVs are released by all cell types and pass through the blood-brain-barrier, providing a proxy of the brain's biochemistry. We have shown previously that α-synuclein (α-syn) concentration in neuronal- and oligodendroglial-EVs (nEVs and oEVs, respectively) isolated from the serum or plasma of healthy controls (HC), and patients with PD or MSA allowed separating MSA from both HC and PD with high sensitivity and specificity. Here, we measured α-syn phosphorylated at Ser 129 (pS129-α-syn), total tau, and neurofilament light chain (NfL) in subsets of the original cohort to test if they improved the diagnostic power.

Methods: pS129-α-syn and total tau were measured in nEVs and oEVs using electrochemiluminescence ELISA. NfL was measured directly in the serum or plasma using Simoa. A multinomial logistic regression with LASSO variable selection was used to select candidate variables to include in a receiver operating characteristic (ROC) analysis. Separation was assessed using the area under the curve in ROC analysis and prediction error was compared using the Akaike information criterion (AIC).

Results: Levels of pS129-α-Syn in oEVs but not nEVs increased in the order of HC < PD < MSA similar to total α-syn. When oEV pS129-α-syn was added to the multivariable model, the AUC for the separation among all groups was higher, and the AIC suggested a better predictive ability, compared to the baseline model. Total tau was statistically significantly lower in both nEVs and

oEVs in MSA compared to PD and HC. The average NfL concentration was significantly lower in females in the PD and MSA groups compared to the HC group.

Conclusion: Addition of pS129-α-syn to total α-syn measured in CNS-originating EVs may improve the differential diagnostic accuracy for synucleinopathies. pS129-α-syn and tau levels in the different groups provide insight into the pathological processes underlying these diseases.

Introduction

Synucleinopathies are neurodegenerative diseases characterized by accumulation of misfolded α-synuclein (α-syn) inclusions in neuronal and/or glial cells. Different synucleinopathies may affect different brain regions and cell types. In Parkinson's disease (PD) and dementia with Lewy bodies (DLB), α-syn deposits predominantly in neuronal Lewy bodies (LBs) and Lewy neurites (LNs), whereas in multiple system atrophy (MSA), α-syn-rich glial cytoplasmic inclusions (GCIs) are found in oligodendrocytes [1, 2]. Despite differences in the underlying pathophysiology, synucleinopathies often are misdiagnosed, especially by non-experts in the early-stages, due to the overlapping clinical symptoms [3-6].

A definite diagnosis of synucleinopathies can only be determined through a neuropathological examination after death [7]. ~15% of patients diagnosed clinically antemortem with PD do not meet the pathological criteria for the disease [6]. The diagnostic accuracy was found to improve from just 53% at ≤ 5 years from symptom onset to 85% at 5–13 years after the initial diagnosis [4]. A 2016 meta-analysis concluded that clinical diagnosis accuracy for PD had not improved in the previous 25 years [8]. In rarer diseases, such as MSA, antemortem misdiagnosis rates are higher [5]. An autopsy study of 134 patients diagnosed with MSA found 71% accuracy in patients diagnosed with probable MSA and 60% in those diagnosed with possible MSA [9]. Thus, an urgent need exists for reliable, sensitive, specific, and minimally invasive biomarkers for synucleinopathies that will allow early diagnosis providing the opportunity to initiate experimental therapy at a meaningful stage of the disease and serve as a screening tool to ensure inclusion of the correct patient population in each clinical trial.

Biomarker discovery using cerebrospinal fluid (CSF) and imaging modalities such as PET, SPECT, or MRI has been the state of the art for neurodegenerative diseases, including

synucleinopathies. However, these strategies are limited by their invasive and/or expensive nature, their low diagnostic power for synucleinopathies, lack of reproducibility among studies, and the need for high level of expertise and/or sophisticated technologies [10-14]. Skin biopsies are promising for distinguishing synucleinopathies from non-synucleinopathies with overlapping symptoms [15, 16] yet are considered more invasive than a blood test and do not show sensitive and specific separation among synucleinopathies. Direct measurements of candidate diagnostic biomarkers for synucleinopathies in serum or plasma has not shown promising results [17-19]. A previous study [20] measured neurofilament light chain (NfL) in blood as a general biomarker for neurodegeneration [21] and showed significantly higher levels in patients with MSA compared to those with PD, suggesting that serum/plasma NfL could be part of a biomarker panel for distinguishing between these diseases.

An alternative approach is the measurement of biomarkers in extracellular vesicles (EVs) originating in the CNS and isolated from the blood [19, 22]. EVs are small vesicles including exosomes, microvesicles, oncosomes and apoptotic bodies [23]. They carry proteins, carbohydrates, lipids and nucleic acids representing their cell of origin. Exosomes are the smallest and most abundant EVs, ranging in diameter between 30 and 200 nm and are thought to communicate cell-state-specific content (e.g., stimulated, differentiated, stressed) with both neighboring and distant cells [24]. In synucleinopathies and other neurodegenerative proteinopathies EVs carry pathological forms of the proteotoxic proteins, e.g., α-syn oligomers, presumably to remove them and protect the cells from further damage [25-27]. The EVs can cross the blood-brain-barrier (BBB) into the blood and protect candidate biomarkers from enzymatic degradation. Thus, measuring cell-state specific biomarkers in CNS-originating EVs isolated from the blood provides a useful window into the brain's biochemistry [28].

Several studies have demonstrated the utility of measuring α-syn in neuronal EVs (nEVs) as a diagnostic biomarker for PD [19, 29-31] and for distinguishing between PD and MSA [32-34]. Recently, our group has shown that α-syn measured in both nEVs and oligodendroglial EVs (oEVs) in the same samples, and in particular the oEV:nEV α-syn concentration ratio, yielded a discriminative formula distinguishing between PD and MSA with 89.8% sensitivity and 86.0% specificity and between healthy controls (HC) and MSA with 96.0% sensitivity and 84.3% specificity [35]. In contrast, the same formula offered moderate separation between PD and HC – 71.4% sensitivity and 62.7% specificity. Here, using remaining samples from the previous study, we evaluated whether adding nEVs and oEVs pS129-α-syn, total tau, tau phosphorylated at Thr 181 (pT181-tau), and/or serum/plasma NfL to the previously measured α-syn might improve the diagnostic power when added to the discriminative formula. To our knowledge, our study is the first to measure pS129-α-syn in nEVs and oEVs and the first to assess tau concentrations in these types of EVs from patients with MSA. Our results show that adding pS129-α-syn concentration levels to the previously reported biomarker panel improves the separation among the three groups, and addition of NfL improves the separation between HC and PD.

Materials and Methods

Patient samples

All the samples used were subsets of those described previously [35]. The determination of diagnosis and methods of sample collection and preparation were described previously. Demographic and clinical characteristics and the number of samples analyzed per group for each biomarker are summarized in Tables 1–3. Due to the limited sample volumes available, for most samples we measured only one or two of the biomarkers and therefore each one was added to the discriminative formula separately.

EV isolation and immunocapture

To remove intact cells and cell-debris, samples were centrifuged at 4 °C for 10 min at 3,400 *g*. Further isolation of nEVs and oEVs was done as described previously [35]. Experimenters were blinded to the diagnosis, demographic data, or any other identifying information.

CD81 measurement

The exosome concentration was estimated using the ExoELISA Ultra CD81 assay (System Biosciences) following the manufacturer's instructions as described previously [35].

pS129-α-syn assay

We used a new in-house-developed electrochemilumiscence ELISA (ECLIA) based on Meso Scale Discovery (MSD)'s platform. The assay has been described in detail in [36].

Total tau and pT181-tau measurement

Total tau and pT181-tau were measured using S-PLEX Human Total Tau or pT181-tau kits, respectively (MSD). Briefly, 50 µL of biotinylated human tau or pT181-tau capture antibodies were added to single-small spot streptavidin-coated wells and incubated at room temperature (RT) with shaking for 1 h at 700 rpm. After washing the plate using 150 µL wash buffer (WB: 0.05% (v/v) Tween-20 in 1X PBS, pH 7.4) per well thrice, 25 µL of blocking buffer and either sample or calibrator were added to each well and allowed to incubate at RT for 1.5 h with shaking at 700 rpm. The wells again were washed thrice using the WB, and 50 µL TURBO-BOOST human tau detection antibody was added to each well and incubated for 1 h with shaking at 700 rpm. The plate was washed thrice using the WB and incubated with 50 µL enhancing solution at RT for 30 min with shaking at 700 rpm. Each well then was washed thrice with WB and 50 µL of TURBO-TAG enhancing solution was added to each well and incubated at 27 °C for 1 h with shaking at

700 rpm. Lastly, the plate was washed thrice using WB, 150 µL of MSD Gold Read Buffer B was added to each well, and the plate was read immediately using a QuickPlex SQ 120 instrument. The data were analyzed using Discovery Workbench 4.0 and quantified with reference to freshly prepared total tau or pT181-tau standard curves.

The reported lower limit of detection (LLoD) of the S-PLEX total tau kit is 0.012 pg/mL and that of the pTau181-tau kit is 0.077 pg/mL. In our hands, the experimental LLoDs were 0.014 and 0.019 pg/mL, respectively, for these assays. The intra- and inter-assay coefficients of variation (CVs) for total tau measurements were 9.2% and 2.9%, respectively. We did not determine CVs for the pTau181-tau kit.

NfL measurement by Single Molecule Array (Simoa)

NfL was measured directly in the serum or plasma samples. Samples were thawed once for aliquoting before measurements, diluted 1:20 (20 µL) in PBS (380 µL) containing a protease and phosphatase inhibitor cocktail (Halt™ Protease and Phosphatase Inhibitor Cocktail, ThermoFisher Scientific), and analyzed by UCLA's Immunogenetics Center using Simoa NfL kits (Quanterix) on an HD-X Analyzer (Quanterix).

Statistical analysis

One-way comparisons for the biomarkers between the groups were conducted using the Kruskal-Wallis test. Sample concentrations that were below the LLoD of the assay were imputed as the minimum value divided by 2 [37]. Correlations across individual biomarkers or between biomarkers and clinical test scores were evaluated using Spearman's method. A multinomial logistic regression model with Least Absolute Shrinkage and Selection Operator (LASSO) variable selection was used to select the best variables to include in logistic models followed by ROC

analysis. Sensitivity and specificity were estimated at the best threshold, defined as the value of the linear predictor in the logistic model which maximized the unweighted sum of the sensitivity and specificity using ROC models for each pairwise combination of groups (HC vs. PD, HC vs. MSA and PD vs. MSA). Prediction error was compared using the Akaike Information Criterion (AIC). Analyses were performed using Prism 9.4 (GraphPad) or R version 4.0.2 (Copyright © 2020 The R Foundation for Statistical Computing). Most results are presented in the figures as log-transformed values to improve normalization and facilitate statistical analysis. Non-transformed values are summarized in Table 4.

Results

pS129-α-syn

The levels of pS129-α-syn in normal adult human brain are ~4% of total α-syn and may increase up to ~90% in LBs [38-40]. pS129-α-syn also is highly enriched in GCIs in the MSA brain, though to a lesser degree than in LBs [40]. These differences suggest that the pS129-α-syn concentrations in nEVs and/or oEVs may help distinguish among the groups.

Measurement of pS129-α-syn in 32 HC, 46 PD, and 30 MSA samples showed that the concentrations in most cases were a small fraction of the total α-syn (Supplementary Fig. S1a). In the nEVs, the pS129-α-syn concentrations trended toward a decrease in the order HC > PD > MSA but the differences were statistically insignificant (Figure 1). In contrast, pS129-α-syn concentrations in oEVs increased in the same order, HC < PD < MSA, and were significantly higher in both disease groups compared to the HC group (Figure 1). These data suggest that EV-mediated removal of pS129-α-syn from neurons is not affected by synucleinopathy, whereas in oligodendrocytes it is increased in MSA and in a subgroup of patients with PD compared to oligodendrocytes in normal, age-matched brains.

The oEV:nEV pS129-α-syn ratio showed a similar behavior, increasing in the order HC < PD < MSA (Supplementary Fig. S1b). In most patients with MSA this ratio was > 1, as reported previously for total α-syn [35]. However, in the PD group roughly equal numbers of samples were < 1 or > 1. Consequently, unlike the oEV:nEV total α-syn ratio, which strongly discriminated between PD and MSA, the same ratio of pS129-α-syn concentration only moderately separated the groups.

Total tau and pT181-tau

Although tau and hyperphosphorylated tau oligomerization and aggregation typically are thought of in the context of Alzheimer's disease and other tauopathies, multiple genome-wide association and other studies investigating genetic risks for idiopathic PD revealed that polymorphisms in the MAPT gene are strongly linked to PD [41-46]. Abnormal tau has been shown in postmortem studies to be abundant in the striatum of patients with PD [47] and tau aggregates have been observed in ~50% of PD brains [48]. In contrast, brain hyperphosphorylated tau pathology only rarely has been reported in patients with MSA [49-51] and in those cases, it might have reflected a co-pathology of AD. Thr 181 is a common phosphorylation site in tau found in various pathological conditions [52-56] and CSF pT181-tau has been used as a biomarker for PD and atypical parkinsonian disorders [57-59].

Total tau was measured in 54 HC, 51 PD, and 41 MSA samples. One sample was excluded from the oEV MSA group because it was 39 standard deviations above the mean. The tau concentrations were approximately an order of magnitude lower than the α-syn concentrations (Table 4), below 1 pg/ml in many of the samples. In a few samples, the signal was below the LLoD and was imputed as the minimum/2 value (Figure 2). The average concentration in both nEVs and oEVs was significantly lower for the MSA group compared to the HC and PD groups, in agreement with the

scarce observation of tau pathology in MSA brain. The HC and PD groups had similar tau concentrations in both nEVs and oEVs. The differences between nEVs and oEVs were statistically insignificant in all three groups (Figure 2), unlike the total α-syn [35] and pS129-α-syn results (Figure 1), suggesting that in contrast to α-syn, the oEV:nEV tau concentration was not useful for distinguishing MSA from HC or PD and that measurement of tau in one type of EV is sufficient.

In our first attempt to measure pT181-tau we isolated nEVs an oEVs from 38 samples (9 HC, 17 PD and 12 MSA). Unfortunately, pT181-tau levels were detectable only in 6 of the 76 EV lysates—one PD and one MSA samples showing detectable pT181-tau concentrations in both nEVs and oEVs, whereas another MSA sample and one HC sample had detectable pT181-tau concentrations in oEVs only. These findings suggest that pT18- tau levels in CNS-originating EVs isolated from the samples used in our study were only a small fraction of the total tau concentration and demonstrate that at the present assay sensitivity levels this analyte is not useful for distinguishing among HC, PD, and MSA.

NfL

Increased concentrations of NfL in the CSF have emerged in recent years as a measure of neuroaxonal injury and neurodegeneration not specific to a particular disease [21, 60, 61]. Several studies have shown that plasma NfL concentrations correlate well with those in the CSF [62-64]. Previously, Hansson et al. reported significantly higher plasma NfL concentrations in patients with MSA compared to HC and patients with PD [20]. Therefore, we tested whether similar differences could be detected in our cohort. An important difference between our measurement and that of Hansson et al. was that they used plasma whereas the majority of our samples were serum. NfL concentrations in serum and plasma have been reported to be strongly correlated in patients with

multiple sclerosis (r = 0.95) [65]. We are not aware of similar side-by-side comparisons in patients with synucleinopathies.

Because the volume needed for the direct measurement of NfL in each sample, 20 μL, is ~10% of the volume needed for EV isolation we could measure NfL in a larger number of samples – 88 HC, 79 PD, and 74 MSA. Unlike the other biomarkers, which were measured using ECLIA, we used Simoa to quantify NfL to match most of the current literature. Our analysis showed a significantly lower average NfL concentration in the PD group compared to both the HC and the MSA groups. The lower concentration of NfL in PD compared to HC samples was in agreement with a recent paper by Chen et al. who reported similar findings in an Asian cohort [66]. Moreover, Chen et al. reported that the lower in NfL plasma concentration was statistically significant only in females. Therefore, we tested if the same phenomenon could be found in our cohort. Indeed, we found lower NfL concentrations in females but not in males, in the PD group, corroborating the findings of the previous study. In contrast to the report by Hansson et al., we did not find significant differences between HC and MSA when both sexes were analyzed together (Figure 3). When males and females were analyzed separately, the NfL concentration in female patients with MSA (270 pg/mL) was significantly lower than in the healthy females (326 pg/mL).

Statistical models

Previously, a multinomial logistic regression (MLR) model with LASSO variable selection performed the best out of four models examined and selected nEV α-syn concentration, the oEV:nEV α-syn concentration ratio, and total EV concentration to create a ROC model that best separated among the HC, PD, and MSA groups [35]. Here, we used the same approach to test whether pS129-α-syn, tau, or NfL might improve the separation when added separately to the previously selected parameters. The number of samples in which both pS129-α-syn and tau could

be measured was too small in the current study to allow meaningful evaluation of both together. NfL was measured in most of the samples and therefore we tested it in combination with pS129-α-syn or tau.

For the subset of samples with pS129-α-syn measurements, as might be expected based on the data presented in Figure 1, the MLR model selected to add oEV pS129-α-syn concentrations to the previous parameters in the ROC model. The addition of pS129-α-syn improved the model predictions compared to the model that did not include oEVs-pS129-α-syn (AIC 136.1 vs 138.7, respectively; AIC change = –2.6). The improved model separated the PD and HC groups with AUC = 0.874, MSA and HC group with AUC = 0.993, and the PD and MSA groups with AUC = 0.936 (Figure 4a). Addition of NfL did not improve the separation in this subset of samples.

For the subset of samples with total tau measurements, the model added oEV tau to the previously selected parameters. However, the addition of this parameter did not result in a significant improvement in the model predictions compared to the model that did not include oEV tau (Figure 4b and Table 5). When NfL was added to oEV tau, there was a significant improvement in model predictions (AIC = 260.8 vs. 263.1; AIC change = –2.2) and the separation between the PD and HC groups in ROC analysis increased compared to tau alone from AUC = 0.633 to 0.720 ($p = 0.055$).

α-Syn concentration in both nEVs and oEVs in all the groups combined together correlated positively with oEV pS129-α-syn ($r_{nEV} = 0.38$, $r_{oEV} = 0.35$; $p < 0.0001$) but not with nEV pS129-α-syn. To assess the contribution of the different groups to these correlations we tested them in each group separately. In the control group, no significant correlation was found between nEVs or oEVs total α-syn and nEVs or oEVs pS129-α-syn indicating that this group did not contribute to the observed correlations. In the PD group, both nEVs and oEVs α-syn correlated positively with

oEVs pS129-α-syn (r_{nEV} = 0.37, p = 0.010; r_{oEV} = 0.33, p = 0.025). Similarly, positive correlations were found also for the MSA group (r_{nEV} = 0.38, p = 0.037; r_{oEV} = 0.38, p = 0.036). None of the biomarkers correlated with disease duration or disease progression as assessed by Unified Parkinson's Disease Rating Scale-III (UPDRS-III), Unified Multiple System Atrophy Rating Scale (UMSARS), or Hoehn and Yahr scale (H&Y).

Discussion

Correct diagnosis of synucleinopathies is crucial for multiple reasons. Symptomatic treatment, e.g., dopaminergic replenishment with levodopa, is effective for managing the motor symptoms of patients with PD, especially in early stages [67], but not in patients with MSA and may worsen cognitive symptoms in DLB. MSA is a more aggressive disease compared to PD, leading to a rapid deterioration of motor and autonomic functions, and death on average eight years from symptom onset. Medical management of MSA differs from PD in medication adjustment, side-effect examination, and monitoring of potential common complications including urinary retention, sleep apnea, and aspiration. Thus, patients' and caregivers' emotional and practical responses to the diagnosis of MSA compared to PD differ substantially. Lifestyle decisions that depend on knowing the diagnosis, including diet and exercise, can have a major impact on disease course and quality of life [68-71] and accurate diagnosis and prognosis help patients manage their advanced care decisions.

Early diagnosis will enrich recruitment of subjects for research studies, which is a major difficulty in MSA research. Critically, effective development of disease-modifying therapy for these diseases requires establishing inclusion and exclusion criteria for clinical trials based not only on the symptoms, which even in the best-controlled trials are highly variable, but also on the underlying pathology. Candidate biomarkers measured in CNS-originating EVs are attractive thanks to the

non-invasive nature of the needed blood test and the ability to compare the biomarkers in EVs from different cell types.

Previously, we showed that α-syn concentration in nEVs and oEVs isolated from HC, PD, or MSA blood samples separated MSA from the HC and PD groups with high sensitivity and specificity. Here, using the same strategy, we found that pS129-α-syn further improves the predictions (Figs. 1 and 4a, Table 5), most notably between HC and PD, suggesting that the combination of total and pS129-α-syn could be multiplexed in the future to create a test assisting clinicians in the differential diagnosis. To our knowledge, our study is the first to measure pS129-α-syn as a potential biomarker in CNS-originating EVs for the separation among HC, PD, and MSA, and tau in nEVs and oEVs in patients with MSA. Although total tau (Fig. 2) showed significant differences among the groups, the concentration distributions overlapped substantially and this biomarker did not improve the separation. When both NfL and oEVs tau were added to the model, their combination improved the separation between the HC vs PD groups above the baseline model, though to a lower extent than pS129-α-syn. The concentrations of the fourth biomarker we tested, pT181-tau, were mostly below the detection limit of the assay we used, 0.019 pg/ml.

Several studies have assessed the potential of pS129-α-syn measurements directly in the CSF or plasma as a potential biomarker for synucleinopathies [72-77]. The results were highly variable, and in particular, some of the studies did not detect pS129-α-syn in CSF [77, 78], likely because highly sensitive pS129-α-syn assays were not available commercially, resulting in multiple groups developing and using different assays for measuring this candidate biomarker. Like these groups, we used an in-house developed pS129-α-syn assay, which in our case was a new ECLIA [36].

pS129-α-Syn is known to be highly enriched in LBs and LNs, and to a lower extent in GCIs [79].

Interestingly, we found the highest concentration of oEV-associated pS129-α-syn in patients diagnosed with MSA (Fig. 1). Although new studies have begun mapping α-syn proteoforms in different brain regions and different synucleinopathies [80, 81], how much pS129-α-syn exists in the brain of patients with MSA compared to those with PD currently is unknown. Thus, our findings might simply reflect an overall higher putative amount of this proteoform in MSA compared to PD, resulting in higher concentrations in the oEVs. Alternatively, if the amount of pS129-α-syn in the brain is similar in the two diseases or lower in MSA, the higher concentrations we found in the oEVs would suggest an increased secretion of this α-syn form by oligodendroglia in MSA compared to PD, in agreement with its lower abundance in MSA-brain deposits compared to those in the PD brain.

In this context, the observation that the increase in pS129-α-syn was only in the oEVs and not in the nEVs is intriguing. In both diseases neurons are thought to use EVs to expel excess α-syn and pS129-α-syn to mitigate proteotoxic stress. However, whereas total α-syn concentration in nEVs increases significantly in the order HC < PD < MSA, pS129-α-syn shows an opposite trend. This phosphorylated form of α-syn has a substantially higher tendency to aggregate than the unphosphorylated protein and thus may be retained inside the cells, especially in LBs and LNs, and to a lower extent in GCIs. The significantly higher concentrations of pS129-α-syn in the oEVs from the patients, particularly those with MSA, compared to the HC group may result from the different cellular environment in oligodendrocytes compared to neurons [79] and/or the different α-syn strains formed in PD and MSA [82].

Another putative explanation is that nEVs containing pS129-α-syn are taken up by glial cells, including oligodendrocytes, for processing and degradation. This process appears to work

efficiently in the healthy brain, but presumably fails in most patients with MSA (Figure 1), possibly due to reduced levels of Coq2, Coq7, and ATP [83].

Despite the strong PD risk associated with MAPT polymorphism and the frequent findings of tau aggregates in the same brain areas where Lewy bodies deposit, our data showed no difference between tau concentrations in nEVs or oEVs from HC and PD samples, but were significantly lower in the MSA group (Figure 2). The lack of difference between the HC and PD groups suggests that unlike α-syn, the PD brain does not sense tau accumulation as threatening and therefore neither the neurons nor the glia attempt to remove excess tau via EVs. In contrast, the lower concentrations in the CNS-originating EVs from patients with MSA suggest a possible disruption of tau expression and/or its trafficking into EVs in this disease.

Tau co-pathology in MSA has been reported rarely. Giasson et al. probed the GCIs of 21 MSA brains using a polyclonal anti-tau antibody that recognizes all alternatively spliced forms of tau, independent of phosphorylation, and found tau only in a few GCIs [84]. Another clinico-pathological study of seven MSA cases did not find tau inclusions in oligodendroglial GCIs, but rather found tau-positive GCIs in astrocytes [49]. A recent study using monoclonal antibody AT8 in 14 patients with MSA found weak presence of granular positive tau-inclusions in five of these patients exclusively in the cerebral white matter [85]. These five patients were long-survivors of MSA, suggesting a link between tau co-pathology in MSA and longevity. These observations speak against retention of aggregated tau in the MSA brain as the reason for the reduced concentration in the CNS-originating EVs.

The use of CNS-originating EVs to distinguish among parkinsonian disorders has focused mainly on α-syn [18, 33, 34, 86, 87], sometimes in combinations with other markers, e.g., Clusterin. CSF tau has been used as a biomarker in synucleinopathies primarily in the context of cognitive decline

[88, 89], yet a few studies also have assessed the use of tau as a biomarker in nEVs from patients diagnosed with PD. Shi et al. immunoprecipitated nEVs directly from the plasma of 91 patients with PD, 106 patients with AD, and 196 age- and sex-matched HC and measured tau concentrations using a Simoa assay [29]. They showed that the concentrations were higher in PD than in the AD and HC groups, though the separation between PD and HC was low (AUC = 0.607). In agreement with the lack of difference we found between patients with PD and HC in nEV tau, Blommer et al. isolated nEVs from 271 participants (103 PD, 81 PD with mild cognitive impairment (PD-MCI), 40 PD dementia (PDD), and 49 HC) and did not find differences between the groups in nEV-tau concentrations quantified using an EMD Millipore multiplexed magnetic bead assay [90]. In contrast to our findings, Blommer et al. reported higher pT181-tau concentrations in both cognitively impaired (MCI and PDD) and cognitively normal patients with PD compared to HC, and higher concentrations in the PD-MCI and PDD groups than in cognitively normal PD. ROC analyses revealed low-to-moderate separation among the groups using the combinations of pTau181, α-syn, Aβ42, pY-IRS-1, pmTOR and pSer312-IRS-1 (AUC range: 0.57-0.71) [90].

The most likely reason for Blommer et al.'s success in measuring pT181-tau as opposed to our work is the higher sample volume they used, 500 μL, compared to the 200-μL samples in our study, though the reported sensitivity of the magnetic-bead assay they used, 1.5 pg/mL was lower than that of the ECLIA in our study, 0.019 pg/mL. It is also possible that pT181-tau is more susceptible to degradation over time than the other biomarkers we measured and therefore we only detected it in a few samples.

While these results may seem promising, they are limited by various factors (summarized in Fig. 5). The results from our study [91] showed high overlap in the data, as can be seen in the error bars

in Fig 1a, with an approximately equal number of samples, which suggests that the results may not be significant [92]. Further, in another subset of samples, measured ~2.5 years later, pS129-α-syn in CNS-originating EV lysates resulted in signals below the lower limit of detection (LLoD) of the assay. This may suggest the protein had deteriorated over time but may also suggest that batch-to-batch variability due to the 2.5-year gap between measurements led to confounding results as suggested by Lashuel et al. [93].

The pS129-α-syn measurements were conducted using an in-house ECLIA with an antibody highly specific for pS129-α-syn (EP1536Y) for capture and the SULFO-TAG anti-α-syn antibody provided by Meso Scale Discovery for detection. However, looking at Fig. 3 in Chapter 1, we observed poor dilution linearity and spike recovery results, indicating that the levels of pS129-α-syn in patients with PD and MSA or HCs found in our study may have been due to a matrix effect. Although we have shown that the anti-pS129-α-syn EP1536Y antibody is highly specific for pS129-α-syn (as seen in Fig. 1; Dutta et al., 2023a), these findings suggest caution is needed when interpreting the results from the ECLIA assay which may work in serum samples only with the possibility of confounding matrix effects, but not plasma or CSF.

Although pS129-α-syn is commonly targeted as a marker of synucleinopathies, α-syn is also prone to concomitant post-translational modifications and C-terminal truncations [93, 94]. This led the group of Lashuel et al. [93] to investigate how these issues may impact various antibodies specific for pS129-α-syn. Their findings suggest that the EP1536Y antibody is susceptible to cross-reactivity with other proteins, fails to recognize pS129-α-syn truncated at either the 133 or 135 residues, shows reduced signal for pS129/nY125/nY133/nY136-α-syn fibrils compared to pS129-α-syn fibrils, and fails to robustly detect pS129-α-syn in Western blots. These findings suggest that the results seen with nEVs and oEVs pS129-α-syn in patients with PD, MSA, and HC are not

reliable until further characterization is done. Moreover, this particular antibody may react with the antibodies used for capturing nEVs and oEVs as seen with the α-synuclein antibody [95].

We use a two-step procedure to capture CNS-originating EVs, first by using a polymer-based precipitation technique followed by immunocapture of nEVs or oEVs using the anti-L1CAM or anti-MOG antibody, respectively. Our group had not characterized pS129-α-syn levels directly in the serum/plasma or directly in the EV isolated bulk before immunocapture, limiting the interpretation of results. Lastly, it is unclear why the LASSO model selected oEVs pS129-α-syn to improve separation among the groups, especially patients with PD and MSA, given that it was not significantly different between the two diseases ($p = 0.52$), which is supported by a meta-analysis [96].

On the other hand, tau has been linked to PD pathology. Thus, our team has attempted to measure nEVs and oEVs tau, and the findings did not suggest improved separation among the groups with high overlap and many samples being below the LLOD of the assay. As this is a commercial assay, we did not further characterize it in our laboratory. Similar to the above, we had not measured tau directly in serum/plasma or in bulk EVs isolated [91]. Furthermore, we obtained no signals for the measurements of pT181-tau in nEVs and oEVs of patients with PD, MSA and HCs as well as another subset of patients with tauopathies.

Another critical point that we did not address is the control of the preanalytical variables and how they may impact the purity, property, number and content of EVs isolated. Many studies have shown that preanalytical variations such as the time from blood collection to the first centrifugation at various temperatures, centrifugation force and time, depletion of platelets, the number of freeze/thaw cycles before EV isolation, choice of anticoagulation agent mixed with plasma, the time of preparation, centrifugation methodology, the nature of transport, number of freeze/thaw

cycles, storage conditions, temperature and the type of collection tube have all been shown to influence the purity, property, number and content of EVs isolated [97-103]. None of these variables have been controlled in Taha et al., further indicating that the results might be due to chance which explains (see below) why other groups have failed to replicate these findings. Specifically, in Taha et al., we did not perform subgroup analyses by repository due to small n, even though different biobank repositories do indeed have different protocols. It is also important to note that the technique used here is of high cost and requires approximately 3 days to obtain lysates of CNS-originating EVs from the blood.

Current efforts by ISEV [104] and others [105, 106] are aiming toward more rigorous standardization so that findings in EVs can be replicated successfully. All studies measuring biomarkers in CNS-originating EVs for parkinsonian disorders [29, 30, 107-115] are encouraged to keep detailed record of their methodology and handling steps through EVTRACK [116].

A technical limitation shared by most studies using CNS-originating EVs for biomarker analysis is that the minute amount of material often does not allow confirming the cellular origin of the EVs using independent markers. Two recent studies used the same antibody we did for the isolation of nEVs, anti-L1CAM clone 5G3 and corroborated the neuronal origin of the EVs by demonstrating enrichment of neuronal markers. Kluge et al. used large plasma volumes and demonstrated by western blots that the immunoprecipitated nEVs were enriched in synaptophysin and neuron-specific enolase [31]. Blommer et al. used fluorescence microscopy to visualize EVs double-immunolabelled for L1CAM and the neuronal marker Vamp2. Both studies support the enrichment of nEVs by immunoprecipitation using the 5G3 antibody [90].

Finally, there are three more critical points to take into consideration when interpreting the results. First, other groups have tried to replicate our findings and were not successful. Second, few of the

patients included in the original sample cohort have passed away, and neuropathological diagnosis showed a different diagnosis from the one obtained premortem. Third, the findings in the latest study [91] have not been validated in an independent cohort while no study to date replicated the findings in the original study [35], further weakening the appropriate interpretation of the results.

orated the neuronal origin of the EVs by demonstrating enrichment of neuronal markers. Kluge et al. used large plasma volumes and demonstrated by western blots that the immunoprecipitated nEVs were enriched in synaptophysin and neuron-specific enolase [31]. Blommer et al. used fluorescence microscopy to visualize EVs double-immunolabelled for L1CAM and the neuronal marker Vamp2. Both studies support the enrichment of nEVs by immunoprecipitation using the 5G3 antibody [90].

Current efforts by ISEV [104] and others [105, 106] are aiming toward more rigorous standardization so that findings in EVs can be replicated successfully. All studies measuring biomarkers in CNS-originating EVs for parkinsonian disorders [29, 30, 107-115] are encouraged to keep detailed record of their methodology and handling steps through EVTRACK [116].

Conclusion

In a sample cohort we used previously for measuring α-syn in nEVs and oEVs, we tested whether the addition of nEV/oEV pS129-α-syn, total tau, pTau181-tau, or serum/plasma NfL could help distinguish among HC, PD, and MSA. We found that the addition of oEV pS129-α-syn to the MLR model improved the predictions among the groups. Tau concentrations in both types of EVs were significantly lower in MSA than in HC or PD but did not improve the predictions. The levels of pT181-tau were for the most part below the detection limit of the assay. NfL was statistically significantly lower in the PD group compared to the other groups. NfL on its own did not improve the separation, but when added to the model with oEVs tau, it improved the separation between

the HC and PD groups. Our initial findings need to be validated in larger cohorts and possibly combined with additional recently discovered biomarkers, such as Clusterin [34], amplified fibrillar α-syn [31, 118], and certain miRNAs [119-124]. Moreover, as parkinsonian symptoms are also present in patients with other synucleinopathies, i.e., DLB, and tauopathies, such as progressive supranuclear palsy and corticobasal syndrome, our results may contribute to the establishment of a biomarker panel for improved diagnosis of these disorders.

FIGURES

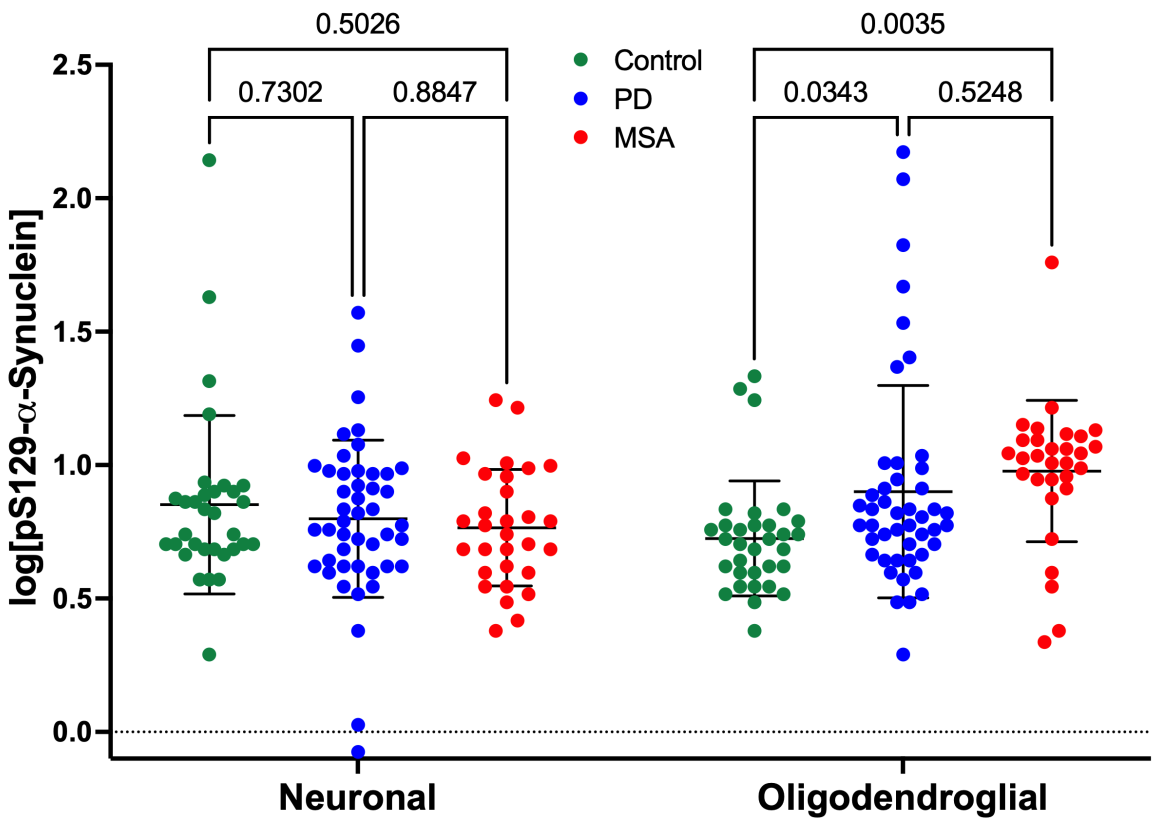

Figure 1. pS129-α-syn concentrations in oEVs but not nEVs differ significantly among the groups. pS129-α-Syn concentrations were measured using ECLIA, log-transformed, and analyzed by a mixed-effect analysis with post-hoc Tukey test. Data are represented as mean ± SD.

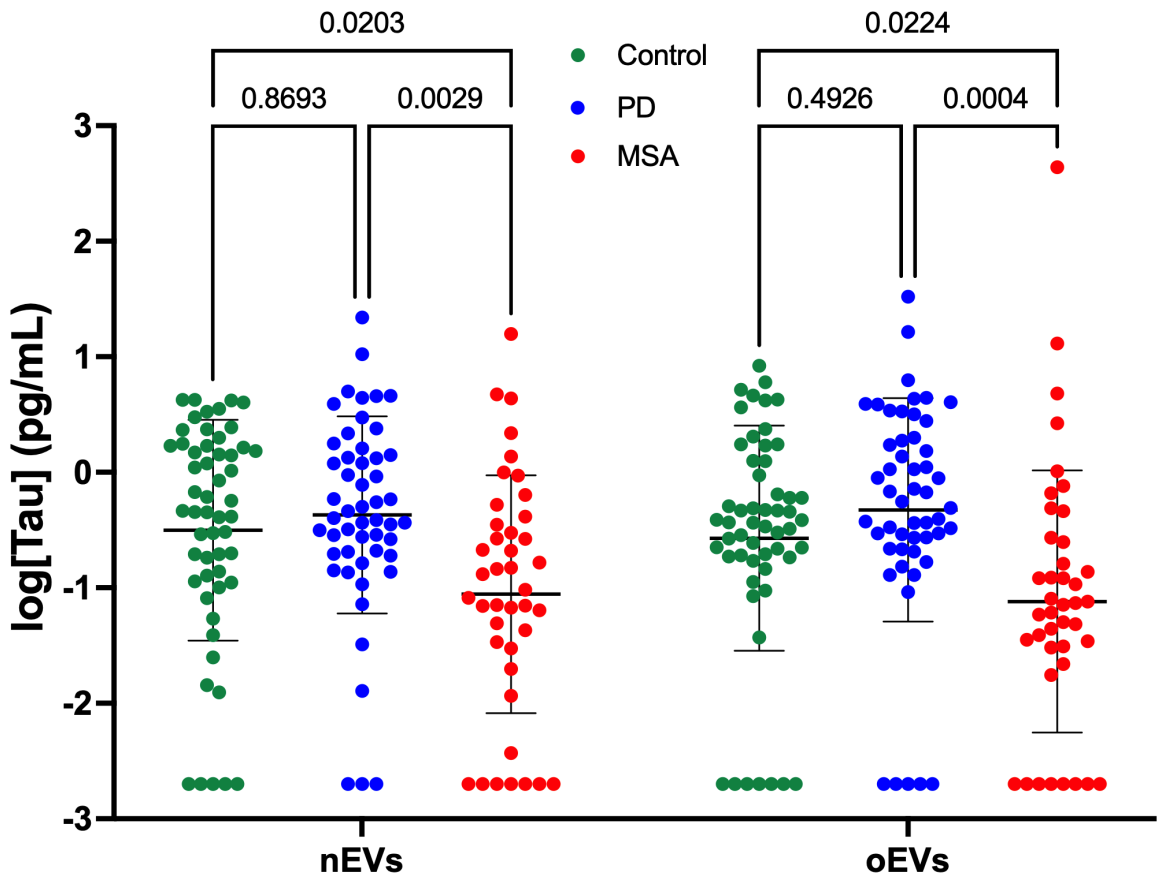

Figure 2. Tau concentration in nEVs and oEVs is significantly lower in MSA than in HC or PD. Tau concentrations were measured using ECLIA, log-transformed, and analyzed by a mixed-effect analysis with post-hoc Tukey test. Data are represented as mean ± SD. Values below the lower limit of detection (LLoD) were imputed as the minimum value divided by 2 [125].

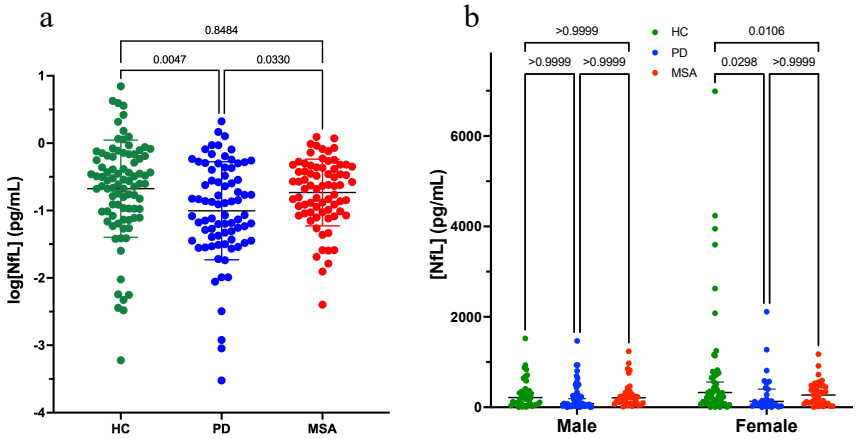

Figure 3. NfL concentration measured in serum/plasma. A) NfL concentrations were measured using Simoa, log-transformed, and analyzed by a one-way ANOVA with post-hoc Tukey test. Data are represented as mean ± SD. **B)** NfL concentrations are lower in the disease groups in females but not males.

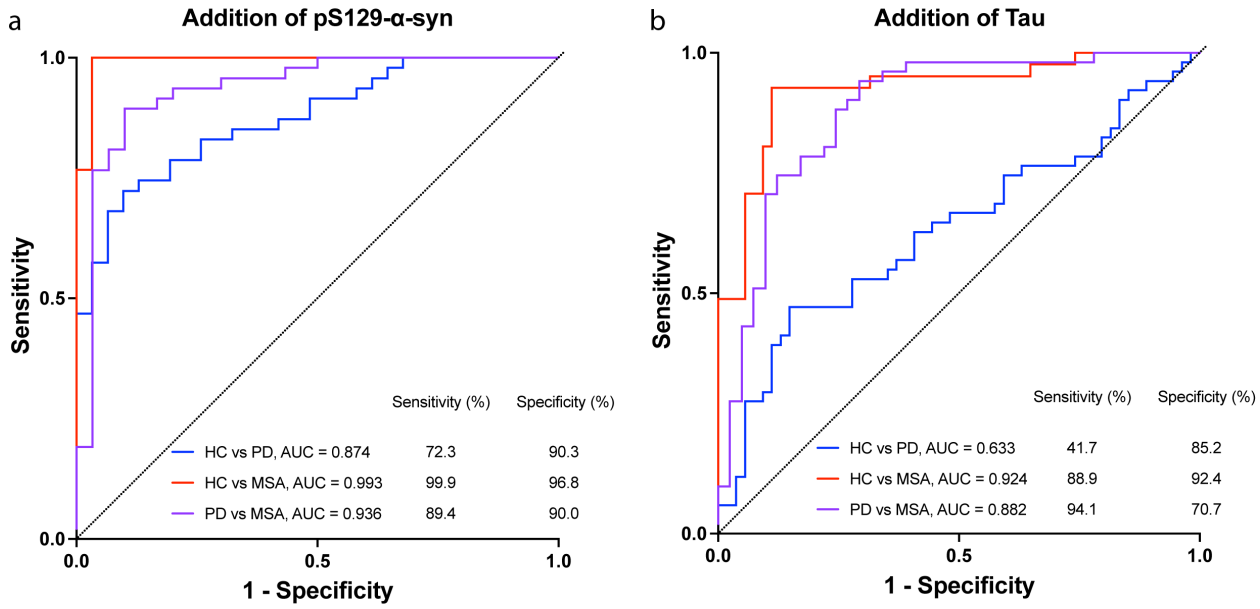

Figure 4. ROC analyses of biomarker concentrations using a multinomial logistic regression model with LASSO variable selection. The model included nEVs α-syn concentration, oEVs:nEVs α-syn concentration ratio, total EV concentration in the sample and (a) oEV pS129-α-syn concentration or (b) oEVs tau concentration

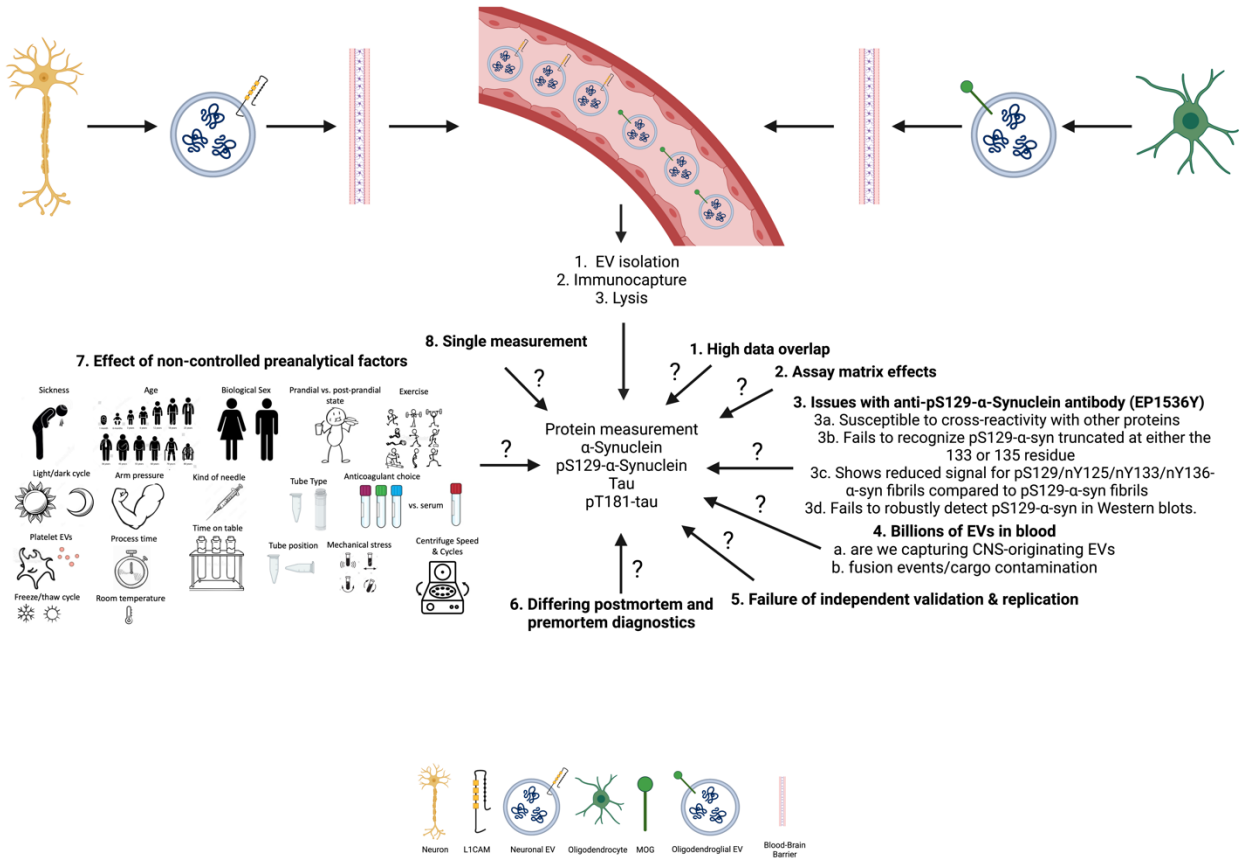

Figure 5. Limitation of the current efforts for measuring biomarkers in CNS-originating EVs for the differential diagnosis of Parkinson's disease and multiple system atrophy.

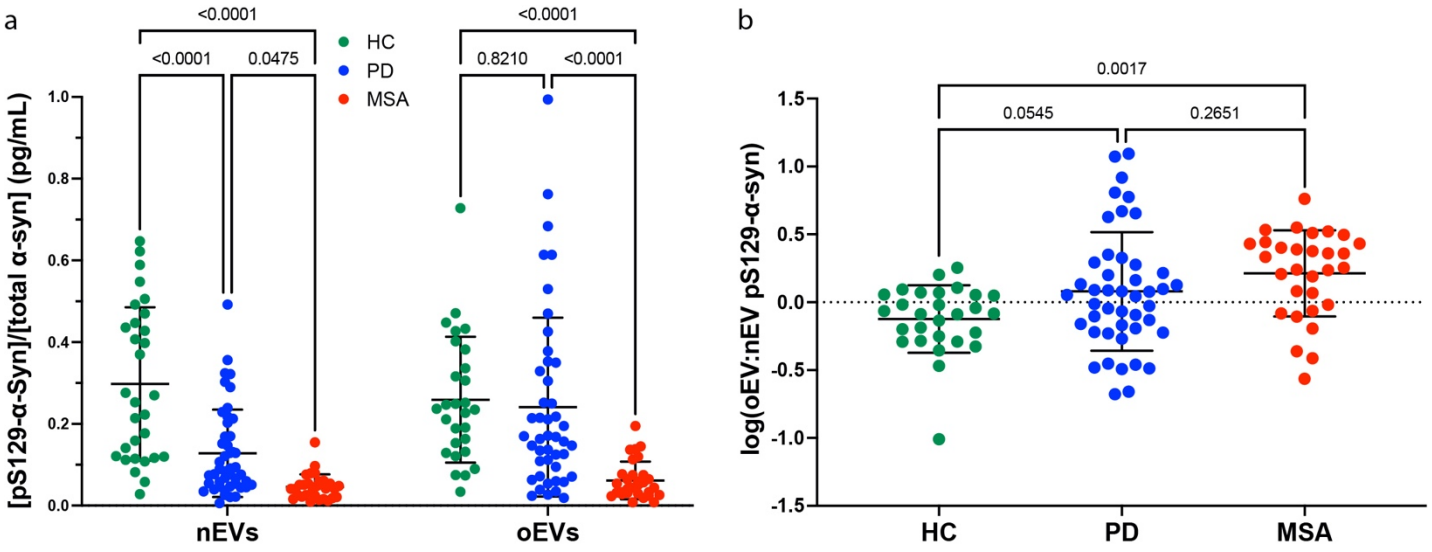

Supplementary Figure S1. Ratios between pS129-α-syn and total α-syn concentrations and between pS129-α-syn concentrations in oEVs and nEVs. a) Ratio between the concentrations of pS129-α-syn and total α-syn in each type of EV. P-values were calculated using a mixed model in Prism 9.4 (GraphPad). The apparent decrease in the order HC > PD > MSA reflects the fact that the differences in total α-syn concentration are larger than those in pS129-α-syn. b) Ratio between pS129-α-syn measured in oEVs and nEVs in each sample. P-values were calculated using a one-way ANOVA.

Table 1. Demographic and clinical characteristic of the patients whose samples were used for pS129-α-syn measurements.

Variable	All Samples	Control	PD	MSA (C:P)
Total number	109	32	47	30 (26:4)
Age (range)[a]	66.8 ± 11.6 (35-90)	60.2 ± 13.1(35-84)	71.6 ± 9.8 (37-90)	62.7 ± 8.2 (46-79)
Sex (male:female)	58:51	17:15	28:19	13:17
Disease Duration (range)[a]			8.1 ± 5.0 (0-19)	4.4 ± 2.6 (0-10)
Race/ethncity[b]	As[c] - 8	As – 1	As – 0	As – 7
	B - 2	B - 0	B - 1	B - 1
	H - 1	H - 0	H - 0	H - 1
	HN - 14	HN - 6	HN - 8	HN - 0
	NA - 2	NA - 1	NA - 1	NA - 0
	ND - 1	ND - 0	ND - 0	ND - 1
	W - 81	W - 24	W - 37	W - 20
UPDRS[d] (range)			25.1 ± 15.6 (0-59)	
H&Y[d] (range)	2.7 ± 1.1 (1-5)		2.5 ± 1.0 (2-5)	3.8 ± 1.0 (1-5)
MMSE[d] (range)	26.4 ± 6.9 (0-30)		26.3 ± 6.4 (0-30)[e]	26.5 ± 9.3 (0-30)

[a]Mean ± SD. [b]As — Asian; B — Black; H — Hispanic; HN — Hispanic non-White; NA — Native American; ND — non-disclosed; W — White. [c]Korea — 2; Philippines — 1; Taiwan — 1; Vietnam —1; Undefined Asian — 3. [d]UPDRS — Unified Parkinson's disease rating scale; H&Y —Höhn and Yahr rating scale; MMSE —Mini-Mental State Examination. [e]Converted from Montreal Cognitive Assessment (MoCA) according to Lawton et al.

Table 2. Demographic and clinical characteristic of the patients whose samples were used for total tau measurements.

Variable	All Samples	Control	PD	MSA (C:P)
Total number	153	54	51	48 (21:3)
Age (range)[a]	67.1 ± 10.6 (35-90)	64.8 ± 11.0 (35-88)	71.1 ± 10.0 (40-90)	63.7 ± 8.6 (47-79)
Sex (male:female)	58:51	35:16	35:16	31:17
Disease Duration (range)[a]			8.7 ± 4.6 (1-20)	5.7 ± 5.2 (1-26)
Race/ethncity[b]	As[c] - 4	As – 1	As – 1	As – 2
	B - 3	B - 0	B - 1	B - 2
	H - 15	H - 10	H - 5	H - 0
	HN - 8	HN - 4	HN - 4	HN - 0
	NA - 3	NA - 0	NA - 3	NA - 0
	ND - 4	ND - 4	ND - 0	ND - 0
	W - 92	W - 35	W - 37	W - 20
UPDRS[d] (range)			12.6 ± 1.0 (0-5)	
H&Y[d] (range)	2.78 ± 1.1 (0-5)		2.5 ± 1.0 (2-5)	4.5 ± 0.6 (4-5)
MMSE[d] (range)	26.1 ± 5.7 (0-30)		26.3 ± 5.0 (1-30)[e]	24.9 ± 8.4 (0-30)

[a]Mean ± SD. [b]As — Asian; B — Black; H — Hispanic; HN — Hispanic non-White; NA — Native American; ND — non-disclosed; W — White. [c]Korea — 0; Philippines — 0; Taiwan — 0; Vietnam —0; Undefined Asian — 4. [d]UPDRS — Unified Parkinson's disease rating scale; H&Y —Höhn and Yahr rating scale; MMSE —Mini-Mental State Examination. [e]Converted from Montreal Cognitive Assessment (MoCA) according to Lawton et al.

Table 3. Demographic and clinical characteristic of the patients whose samples were used for neurofilament light chain (NfL) measurements.

Variable	All Samples	Control	PD	MSA (C:P)
Total number	241	88	79	74 (56:18)
Age (range)[a]	67.0 ± 10.2 (35-90)	66.4 ± 10.0 (35-88)	72.0 ± 10.3 (37-90)	62.5 ± 7.7 (46-79)
Sex (male:female)	125:116	40:48	51:27	34:40
Disease Duration (range)[a]	6.9 ± 4.4 (0-26)		8.6 ± 4.4 (0-20)	5.1 ± 3.7 (0-26)
Race/ethncity[b]	As[c] - 16	As – 2	As – 1	As –13
	B - 5	B - 0	B - 0	B - 5
	H - 24	H - 13	H - 9	H - 2
	HN - 10	HN - 4	HN - 6	HN - 0
	NA - 8	NA - 3	NA - 5	NA - 0
	ND - 7	ND - 5	ND - 0	ND - 2
	W - 171	W - 61	W – 58	W - 52
UPDRS[d] (range)			24.4 ± 13.6 (0-50)	
H&Y[d] (range)	2.9 ± 0.9 (0-5)		2.4 ± 0.8 (0-5)	3.6 ± 1.3 (1-5)
MMSE[d] (range)	28.0 ± 3.4 (0-30)		27.0 ± 4.3 (0-30)[e]	28.3 ± 1.6 (24-30)

[a]Mean ± SD. [b]As — Asian; B — Black; H — Hispanic; HN — Hispanic non-White; NA — Native American; ND — non-disclosed; W — White. [c]Korea — 2; Philippines — 1; Taiwan — 1; Vietnam — 1; Undefined Asian — 11. [d]UPDRS — Unified Parkinson's disease rating scale; H&Y —Höhn and Yahr rating scale; MMSE —Mini-Mental State Examination. [e]Converted from Montreal Cognitive Assessment (MoCA) according to Lawton et al.

Table 4. Serum/plasma nEV and oEV biomarker measurements for the HC, PD, and MSA groups. All values are reported as median (CI).

Serum/plasma			
Group	HC	PD	MSA
CD81 (particles/mL)	6.19×10^{10} (96.5%)	5.00×10^{10} (95.6%)	4.10×10^{10} (95.8%)
NfL (pg/mL)	262 (95.8%)	85.7 (95.8%)	232 (96.6%)
Neuronal EVs			
pS129-α-Synuclein (pg/mL)	6.06 (98.0%)	5.95 (96.0%)	5.72 (95.7%)
Total tau (pg/mL)	0.46 (96.0%)	0.28 (97.1%)	0.30 (96.5%)
Oligodendroglial EVs			
pS129-α-Synuclein (pg/mL)	5.17 (98.0%)	6.39 (96.0%)	10.7 (95.7%)
Total tau (pg/mL)	0.37 (96.0%)	0.30 (97.1%)	0.15 (98.3%)

Table 5. Multinomial logistic regressions with LASSO variable selection for separation among the HC, PD, and MSA groups. AUC — area under the curve

	Control vs. PD			Control vs. MSA			PD vs. MSA		
	AUC	Sensitivity	Specificity	AUC	Sensitivity	Specificity	AUC	Sensitivity	Specificity
Dutta et al. Acta Neuropathol. 2021 – Discovery Cohort	0.762	60.8%	85.7%	0.961	96.7%	89.8%	0.928	82.4%	93.3%
Dutta et al. Acta Neuropathol. 2021 – Validation Cohort	0.610	71.4%	62.7%	0.962	96.0%	84.3%	0.902	89.8%	86.0%
Addition of oEV pS129-α-syn	0.874	72.3%	90.3%	0.993	99.9%	96.8%	0.936	89.4%	90.0%
Addition of oEV tau	0.633	47.1%	85.2%	0.924	88.9%	92.4%	0.882	94.1%	70.7%

[1]The model was created based on the data in this cohort. New models were created using the previous total α-syn and total EV concentration results together with either oEV pS129-α-syn or oEV tau data.

References

[1] Papp MI, Kahn JE, Lantos PL (1989) Glial cytoplasmic inclusions in the CNS of patients with multiple system atrophy (striatonigral degeneration, olivopontocerebellar atrophy and Shy-Drager syndrome). *J Neurol Sci* **94**, 79-100.

[2] Trojanowski JQ, Lee VM (2003) Parkinson's disease and related α-synucleinopathies are brain amyloidoses. *Ann N Y Acad Sci* **991**, 107-110.

[3] Beach TG, Adler CH (2018) Importance of low diagnostic Accuracy for early Parkinson's disease. *Mov Disord* **33**, 1551-1554.

[4] Adler CH, Beach TG, Hentz JG, Shill HA, Caviness JN, Driver-Dunckley E, Sabbagh MN, Sue LI, Jacobson SA, Belden CM, Dugger BN (2014) Low clinical diagnostic accuracy of early vs advanced Parkinson disease: clinicopathologic study. *Neurology* **83**, 406-412.

[5] Skinner TR, Scott IA, Martin JH (2016) Diagnostic errors in older patients: a systematic review of incidence and potential causes in seven prevalent diseases. *Int J Gen Med* **9**, 137-146.

[6] Schrag A, Ben-Shlomo Y, Quinn N (2002) How valid is the clinical diagnosis of Parkinson's disease in the community? *J Neurol Neurosurg Psychiatry* **73**, 529-534.

[7] Tolosa E, Wenning G, Poewe W (2006) The diagnosis of Parkinson's disease. *Lancet Neurol* **5**, 75-86.

[8] Rizzo G, Copetti M, Arcuti S, Martino D, Fontana A, Logroscino G (2016) Accuracy of clinical diagnosis of Parkinson disease: A systematic review and meta-analysis. *Neurology* **86**, 566-576.

[9] Koga S, Aoki N, Uitti RJ, van Gerpen JA, Cheshire WP, Josephs KA, Wszolek ZK, Langston JW, Dickson DW (2015) When DLB, PD, and PSP masquerade as MSA: an autopsy study of 134 patients. *Neurology* **85**, 404-412.

[10] Huppertz HJ, Moller L, Sudmeyer M, Hilker R, Hattingen E, Egger K, Amtage F, Respondek G, Stamelou M, Schnitzler A, Pinkhardt EH, Oertel WH, Knake S, Kassubek J, Hoglinger GU (2016) Differentiation of neurodegenerative parkinsonian syndromes by volumetric magnetic resonance imaging analysis and support vector machine classification. *Mov Disord* **31**, 1506-1517.

[11] Meijer FJ, Aerts MB, Abdo WF, Prokop M, Borm GF, Esselink RA, Goraj B, Bloem BR (2012) Contribution of routine brain MRI to the differential diagnosis of parkinsonism: a 3-year prospective follow-up study. *J Neurol* **259**, 929-935.

[12] Saeed U, Lang AE, Masellis M (2020) Neuroimaging Advances in Parkinson's Disease and Atypical Parkinsonian Syndromes. *Front Neurol* **11**, 572976.

[13] Worker A, Blain C, Jarosz J, Chaudhuri KR, Barker GJ, Williams SC, Brown RG, Leigh PN, Dell'Acqua F, Simmons A (2014) Diffusion tensor imaging of Parkinson's disease, multiple system atrophy and progressive supranuclear palsy: a tract-based spatial statistics study. *PLoS One* **9**, e112638.

[14] Mollenhauer B, Parnetti L, Rektorova I, Kramberger MG, Pikkarainen M, Schulz-Schaeffer WJ, Aarsland D, Svenningsson P, Farotti L, Verbeek MM, Schlossmacher MG (2016) Biological confounders for the values of cerebrospinal fluid proteins in Parkinson's disease and related disorders. *J Neurochem* **139 Suppl 1**, 290-317.

[15] Gibbons CH, Freeman R, Bellaire B, Adler CH, Moore D, Levine T (2022) Synuclein-One study: skin biopsy detection of phosphorylated alpha-synuclein for diagnosis of synucleinopathies. *Biomark Med* **16**, 499-509.

[16] Donadio V, Wang Z, Incensi A, Rizzo G, Fileccia E, Vacchiano V, Capellari S, Magnani M, Scaglione C, Stanzani Maserati M, Avoni P, Liguori R, Zou W (2021) In Vivo Diagnosis of Synucleinopathies: A Comparative Study of Skin Biopsy and RT-QuIC. *Neurology* **96**, e2513-e2524.

[17] Foulds PG, Diggle P, Mitchell JD, Parker A, Hasegawa M, Masuda-Suzukake M, Mann DM, Allsop D (2013) A longitudinal study on α-synuclein in blood plasma as a biomarker for Parkinson's disease. *Sci Rep* **3**, 2540.

[18] Dutta S, Hornung S, Kruayatidee A, Maina KN, Del Rosario I, Paul KC, Wong DY, Duarte Folle A, Markovic D, Palma JA, Serrano GE, Adler CH, Perlman SL, Poon WW, Kang UJ, Alcalay RN, Sklerov M, Gylys KH, Kaufmann H, Fogel BL, Bronstein JM, Ritz B, Bitan G (2021) α-Synuclein in blood exosomes immunoprecipitated using neuronal and oligodendroglial markers distinguishes Parkinson's disease from multiple system atrophy. *Acta Neuropathol*.

[19] Shi M, Liu C, Cook TJ, Bullock KM, Zhao Y, Ginghina C, Li Y, Aro P, Dator R, He C, Hipp MJ, Zabetian CP, Peskind ER, Hu SC, Quinn JF, Galasko DR, Banks WA, Zhang J (2014) Plasma exosomal α-synuclein is likely CNS-derived and increased in Parkinson's disease. *Acta Neuropathol* **128**, 639-650.

[20] Hansson O, Janelidze S, Hall S, Magdalinou N, Lees AJ, Andreasson U, Norgren N, Linder J, Forsgren L, Constantinescu R, Zetterberg H, Blennow K, Swedish Bio Fs

(2017) Blood-based NfL: A biomarker for differential diagnosis of parkinsonian disorder. *Neurology* **88**, 930-937.

[21] Gaetani L, Blennow K, Calabresi P, Di Filippo M, Parnetti L, Zetterberg H (2019) Neurofilament light chain as a biomarker in neurological disorders. *J Neurol Neurosurg Psychiatry*.

[22] Fiandaca MS, Kapogiannis D, Mapstone M, Boxer A, Eitan E, Schwartz JB, Abner EL, Petersen RC, Federoff HJ, Miller BL, Goetzl EJ (2015) Identification of preclinical Alzheimer's disease by a profile of pathogenic proteins in neurally derived blood exosomes: A case-control study. *Alzheimers Dement* **11**, 600-607 e601.

[23] Doyle LM, Wang MZ (2019) Overview of Extracellular Vesicles, Their Origin, Composition, Purpose, and Methods for Exosome Isolation and Analysis. *Cells* **8**.

[24] Gurung S, Perocheau D, Touramanidou L, Baruteau J (2021) The exosome journey: from biogenesis to uptake and intracellular signalling. *Cell Commun Signal* **19**, 47.

[25] Gustafsson G, Loov C, Persson E, Lazaro DF, Takeda S, Bergstrom J, Erlandsson A, Sehlin D, Balaj L, Gyorgy B, Hallbeck M, Outeiro TF, Breakefield XO, Hyman BT, Ingelsson M (2018) Secretion and Uptake of alpha-Synuclein Via Extracellular Vesicles in Cultured Cells. *Cell Mol Neurobiol* **38**, 1539-1550.

[26] Lööv C, Scherzer CR, Hyman BT, Breakefield XO, Ingelsson M (2016) α-Synuclein in Extracellular Vesicles: Functional Implications and Diagnostic Opportunities. *Cell Mol Neurobiol* **36**, 437-448.

[27] Taha H, Kearney B, Bitan G (2022) A minute fraction of α-synuclein in extracellular vesicles may be a major contributor to α-synuclein spreading following autophagy inhibition. *Front Mol Neurosci*.

[28] Mustapic M, Eitan E, Werner JK, Jr., Berkowitz ST, Lazaropoulos MP, Tran J, Goetzl EJ, Kapogiannis D (2017) Plasma Extracellular Vesicles Enriched for Neuronal Origin: A Potential Window into Brain Pathologic Processes. *Front Neurosci* **11**, 278.

[29] Shi M, Kovac A, Korff A, Cook TJ, Ginghina C, Bullock KM, Yang L, Stewart T, Zheng D, Aro P, Atik A, Kerr KF, Zabetian CP, Peskind ER, Hu SC, Quinn JF, Galasko DR, Montine TJ, Banks WA, Zhang J (2016) CNS tau efflux via exosomes is likely increased in Parkinson's disease but not in Alzheimer's disease. *Alzheimers Dement* **12**, 1125-1131.

[30] Niu M, Li Y, Li G, Zhou L, Luo N, Yao M, Kang W, Liu J (2020) A longitudinal study on α-synuclein in plasma neuronal exosomes as a biomarker for Parkinson's disease development and progression. *Eur J Neurol* **27**, 967-974.

[31] Kluge A, Bunk J, Schaeffer E, Drobny A, Xiang W, Knacke H, Bub S, Luckstadt W, Arnold P, Lucius R, Berg D, Zunke F (2022) Detection of neuron-derived pathological α-synuclein in blood. *Brain*.

[32] Yu Z, Shi M, Stewart T, Fernagut PO, Huang Y, Tian C, Dehay B, Atik A, Yang D, De Giorgi F, Ichas F, Canron MH, Ceravolo R, Frosini D, Kim HJ, Feng T, Meissner WG, Zhang J (2020) Reduced oligodendrocyte exosome secretion in multiple system atrophy involves SNARE dysfunction. *Brain*.

[33] Jiang C, Hopfner F, Berg D, Hu MT, Pilotto A, Borroni B, Davis JJ, Tofaris GK (2021) Validation of α-Synuclein in L1CAM-Immunocaptured Exosomes as a Biomarker for the Stratification of Parkinsonian Syndromes. *Mov Disord*.

[34] Jiang C, Hopfner F, Katsikoudi A, Hein R, Catli C, Evetts S, Huang Y, Wang H, Ryder JW, Kuhlenbaeumer G, Deuschl G, Padovani A, Berg D, Borroni B, Hu MT, Davis JJ,

Tofaris GK (2020) Serum neuronal exosomes predict and differentiate Parkinson's disease from atypical parkinsonism. *J Neurol Neurosurg Psychiatry*.

[35] Dutta S, Hornung S, Kruayatidee A, Maina KN, Del Rosario I, Paul KC, Wong DY, Duarte Folle A, Markovic D, Palma JA, Serrano GE, Adler CH, Perlman SL, Poon WW, Kang UJ, Alcalay RN, Sklerov M, Gylys KH, Kaufmann H, Fogel BL, Bronstein JM, Ritz B, Bitan G (2021) α-Synuclein in blood exosomes immunoprecipitated using neuronal and oligodendroglial markers distinguishes Parkinson's disease from multiple system atrophy. *Acta Neuropathol* **142**, 495-511.

[36] Dutta S, Hornung S, Biggs K, Taha H-B, Siddique I, Shahpasand-Kroner H, Lantz C, Herrera-Vaquero M, Stefanova N, Loo JA, Bitan G (2022) Development of a novel electrochemiluminescence ELISA for quantification of α-synuclein phosphorylated at Ser129 in biological samples. Submitted for publication.

[37] Succop PA, Clark S, Chen M, Galke W (2004) Imputation of data values that are less than a detection limit. *J Occup Environ Hyg* **1**, 436-441.

[38] Anderson JP, Walker DE, Goldstein JM, de Laat R, Banducci K, Caccavello RJ, Barbour R, Huang J, Kling K, Lee M, Diep L, Keim PS, Shen X, Chataway T, Schlossmacher MG, Seubert P, Schenk D, Sinha S, Gai WP, Chilcote TJ (2006) Phosphorylation of Ser-129 is the dominant pathological modification of α-synuclein in familial and sporadic Lewy body disease. *J Biol Chem* **281**, 29739-29752.

[39] Fujiwara H, Hasegawa M, Dohmae N, Kawashima A, Masliah E, Goldberg MS, Shen J, Takio K, Iwatsubo T (2002) α-Synuclein is phosphorylated in synucleinopathy lesions. *Nature Cell Biology* **4**, 160-164.

[40] Peng C, Gathagan RJ, Covell DJ, Medellin C, Stieber A, Robinson JL, Zhang B, Pitkin RM, Olufemi MF, Luk KC, Trojanowski JQ, Lee VM (2018) Cellular milieu imparts distinct pathological alpha-synuclein strains in alpha-synucleinopathies. *Nature* **557**, 558-563.

[41] Simon-Sanchez J, Schulte C, Bras JM, Sharma M, Gibbs JR, Berg D, Paisan-Ruiz C, Lichtner P, Scholz SW, Hernandez DG, Kruger R, Federoff M, Klein C, Goate A, Perlmutter J, Bonin M, Nalls MA, Illig T, Gieger C, Houlden H, Steffens M, Okun MS, Racette BA, Cookson MR, Foote KD, Fernandez HH, Traynor BJ, Schreiber S, Arepalli S, Zonozi R, Gwinn K, van der Brug M, Lopez G, Chanock SJ, Schatzkin A, Park Y, Hollenbeck A, Gao J, Huang X, Wood NW, Lorenz D, Deuschl G, Chen H, Riess O, Hardy JA, Singleton AB, Gasser T (2009) Genome-wide association study reveals genetic risk underlying Parkinson's disease. *Nat Genet* **41**, 1308-1312.

[42] Nalls MA, Pankratz N, Lill CM, Do CB, Hernandez DG, Saad M, DeStefano AL, Kara E, Bras J, Sharma M, Schulte C, Keller MF, Arepalli S, Letson C, Edsall C, Stefansson H, Liu X, Pliner H, Lee JH, Cheng R, International Parkinson's Disease Genomics C, Parkinson's Study Group Parkinson's Research: The Organized GI, andMe, GenePd, NeuroGenetics Research C, Hussman Institute of Human G, Ashkenazi Jewish Dataset I, Cohorts for H, Aging Research in Genetic E, North American Brain Expression C, United Kingdom Brain Expression C, Greek Parkinson's Disease C, Alzheimer Genetic Analysis G, Ikram MA, Ioannidis JP, Hadjigeorgiou GM, Bis JC, Martinez M, Perlmutter JS, Goate A, Marder K, Fiske B, Sutherland M, Xiromerisiou G, Myers RH, Clark LN, Stefansson K, Hardy JA, Heutink P, Chen H, Wood NW, Houlden H, Payami H, Brice A, Scott WK, Gasser T, Bertram L, Eriksson N, Foroud T, Singleton AB (2014) Large-scale

meta-analysis of genome-wide association data identifies six new risk loci for Parkinson's disease. *Nat Genet* **46**, 989-993.

[43] Rhodes SL, Sinsheimer JS, Bordelon Y, Bronstein JM, Ritz B (2011) Replication of GWAS associations for GAK and MAPT in Parkinson's disease. *Ann Hum Genet* **75**, 195-200.

[44] Edwards TL, Scott WK, Almonte C, Burt A, Powell EH, Beecham GW, Wang L, Zuchner S, Konidari I, Wang G, Singer C, Nahab F, Scott B, Stajich JM, Pericak-Vance M, Haines J, Vance JM, Martin ER (2010) Genome-wide association study confirms SNPs in SNCA and the MAPT region as common risk factors for Parkinson disease. *Ann Human Genetics* **74**, 97-109.

[45] Pankratz N, Wilk JB, Latourelle JC, DeStefano AL, Halter C, Pugh EW, Doheny KF, Gusella JF, Nichols WC, Foroud T, Myers RH (2009) Genomewide association study for susceptibility genes contributing to familial Parkinson disease. *Human genetics* **124**, 593-605.

[46] Ezquerra M, Pastor P, Gaig C, Vidal-Taboada JM, Cruchaga C, Munoz E, Marti MJ, Valldeoriola F, Aguilar M, Calopa M, Hernandez-Vara J, Tolosa E (2011) Different MAPT haplotypes are associated with Parkinson's disease and progressive supranuclear palsy. *Neurobiol Aging* **32**, 547 e511-546.

[47] Wills J, Jones J, Haggerty T, Duka V, Joyce JN, Sidhu A (2010) Elevated tauopathy and alpha-synuclein pathology in postmortem Parkinson's disease brains with and without dementia. *Exp Neurol* **225**, 210-218.

[48] Zhang X, Gao F, Wang D, Li C, Fu Y, He W, Zhang J (2018) Tau Pathology in Parkinson's Disease. *Front Neurol* **9**, 809.

[49] Nagaishi M, Yokoo H, Nakazato Y (2011) Tau-positive glial cytoplasmic granules in multiple system atrophy. *Neuropathology* **31**, 299-305.

[50] Campese N, Fanciulli A, Stefanova N, Haybaeck J, Kiechl S, Wenning GK (2021) Neuropathology of multiple system atrophy: Kurt Jellinger`s legacy. *J Neural Transm (Vienna)* **128**, 1481-1494.

[51] Bujan B, Hofer MJ, Oertel WH, Pagenstecher A, Burk K (2013) Multiple system atrophy of the cerebellar type (MSA-C) with concomitant beta-amyloid and tau pathology. *Clin Neuropathol* **32**, 286-290.

[52] Bibl M, Mollenhauer B, Lewczuk P, Esselmann H, Wolf S, Otto M, Kornhuber J, Ruther E, Wiltfang J (2011) Cerebrospinal fluid tau, p-tau 181 and amyloid-β38/40/42 in frontotemporal dementias and primary progressive aphasias. *Dement Geriatr Cogn Disord* **31**, 37-44.

[53] Lederer W, Dominguez CA, Popovscaia M, Putz G, Humpel C (2016) Cerebrospinal fluid levels of tau and phospho-tau-181 proteins during pregnancy. *Pregnancy Hypertens* **6**, 384-387.

[54] Llibre-Guerra JJ, Li Y, Schindler SE, Gordon BA, Fagan AM, Morris JC, Benzinger TLS, Hassenstab J, Wang G, Allegri R, Berman SB, Chhatwal J, Farlow MR, Holtzman DM, Jucker M, Levin J, Noble JM, Salloway S, Schofield P, Karch C, Fox NC, Xiong C, Bateman RJ, McDade E (2019) Association of Longitudinal Changes in Cerebrospinal Fluid Total Tau and Phosphorylated Tau 181 and Brain Atrophy With Disease Progression in Patients With Alzheimer Disease. *JAMA Netw Open* **2**, e1917126.

[55] Rojas JC, Bang J, Lobach IV, Tsai RM, Rabinovici GD, Miller BL, Boxer AL, Investigators AL (2018) CSF neurofilament light chain and phosphorylated tau 181 predict disease progression in PSP. *Neurology* **90**, e273-e281.

[56] Vinothkumar G, Krishnakumar S, Riya, Venkataraman P (2019) Correlation between abnormal GSK3β, β Amyloid, total Tau, p-Tau 181 levels and neuropsychological assessment total scores in CKD patients with cognitive dysfunction: Impact of rHuEPO therapy. *J Clin Neurosci* **69**, 38-42.

[57] Constantinides VC, Paraskevas GP, Emmanouilidou E, Petropoulou O, Bougea A, Vekrellis K, Evdokimidis I, Stamboulis E, Kapaki E (2017) CSF biomarkers β-amyloid, tau proteins and a-synuclein in the differential diagnosis of Parkinson-plus syndromes. *J Neurol Sci* **382**, 91-95.

[58] Delgado-Alvarado M, Gago B, Gorostidi A, Jimenez-Urbieta H, Dacosta-Aguayo R, Navalpotro-Gomez I, Ruiz-Martinez J, Bergareche A, Marti-Masso JF, Martinez-Lage P, Izagirre A, Rodriguez-Oroz MC (2017) Tau/α-synuclein ratio and inflammatory proteins in Parkinson's disease: An exploratory study. *Mov Disord* **32**, 1066-1073.

[59] Bjorkhem I, Patra K, Boxer AL, Svenningsson P (2018) 24S-Hydroxycholesterol Correlates With Tau and Is Increased in Cerebrospinal Fluid in Parkinson's Disease and Corticobasal Syndrome. *Front Neurol* **9**, 756.

[60] Preische O, Schultz SA, Apel A, Kuhle J, Kaeser SA, Barro C, Gräber S, Kuder-Buletta E, LaFougere C, Laske C, Vöglein J, Levin J, Masters CL, Martins R, Schofield PR, Rossor MN, Graff-Radford NR, Salloway S, Ghetti B, Ringman JM, Noble JM, Chhatwal J, Goate AM, Benzinger TLS, Morris JC, Bateman RJ, Wang G, Fagan AM, McDade EM, Gordon BA, Jucker M, Allegri R, Amtashar F, Bateman R, Benzinger T, Berman S,

Bodge C, Brandon S, Brooks W, Buck J, Buckles V, Chea S, Chhatwal J, Chrem P, Chui H, Cinco J, Clifford J, Cruchaga C, D'Mello M, Donahue T, Douglas J, Edigo N, Erekin-Taner N, Fagan A, Farlow M, Farrar A, Feldman H, Flynn G, Fox N, Franklin E, Fujii H, Gant C, Gardener S, Ghetti B, Goate A, Goldman J, Gordon B, Graff-Radford N, Gray J, Gurney J, Hassenstab J, Hirohara M, Holtzman D, Hornbeck R, DiBari SH, Ikeuchi T, Ikonomovic S, Jerome G, Jucker M, Karch C, Kasuga K, Kawarabayashi T, Klunk W, Koeppe R, Kuder-Buletta E, Laske C, Lee J-H, Levin J, Marcus D, Martins R, Mason NS, Masters C, Maue-Dreyfus D, McDade E, Montoya L, Mori H, Morris J, Nagamatsu A, Neimeyer K, Noble J, Norton J, Perrin R, Raichle M, Ringman J, Roh JH, Salloway S, Schofield P, Shimada H, Shiroto T, Shoji M, Sigurdson W, Sohrabi H, Sparks P, Suzuki K, Swisher L, Taddei K, Wang J, Wang P, Weiner M, Wolfsberger M, Xiong C, Xu X, Dominantly Inherited Alzheimer N (2019) Serum neurofilament dynamics predicts neurodegeneration and clinical progression in presymptomatic Alzheimer's disease. *Nature Medicine*.

[61] Olsson B, Portelius E, Cullen NC, Sandelius A, Zetterberg H, Andreasson U, Hoglund K, Irwin DJ, Grossman M, Weintraub D, Chen-Plotkin A, Wolk D, McCluskey L, Elman L, Shaw LM, Toledo JB, McBride J, Hernandez-Con P, Lee VM, Trojanowski JQ, Blennow K (2019) Association of Cerebrospinal Fluid Neurofilament Light Protein Levels With Cognition in Patients With Dementia, Motor Neuron Disease, and Movement Disorders. *JAMA Neurology* **76**, 318-325.

[62] Osborn KE, Khan OA, Kresge HA, Bown CW, Liu D, Moore EE, Gifford KA, Acosta LMY, Bell SP, Hohman TJ, Blennow K, Zetterberg H, Jefferson AL (2019)

Cerebrospinal fluid and plasma neurofilament light relate to abnormal cognition. *Alzheimers Dement (Amst)* **11**, 700-709.

[63] Mielke MM, Syrjanen JA, Blennow K, Zetterberg H, Vemuri P, Skoog I, Machulda MM, Kremers WK, Knopman DS, Jack C, Jr., Petersen RC, Kern S (2019) Plasma and CSF neurofilament light: Relation to longitudinal neuroimaging and cognitive measures. *Neurology* **93**, e252-e260.

[64] Li QF, Dong Y, Yang L, Xie JJ, Ma Y, Du YC, Cheng HL, Ni W, Wu ZY (2019) Neurofilament light chain is a promising serum biomarker in spinocerebellar ataxia type 3. *Mol Neurodegener* **14**, 39.

[65] Hendricks R, Baker D, Brumm J, Davancaze T, Harp C, Herman A, Budingen HV, Townsend M, Fischer SK (2019) Establishment of neurofilament light chain Simoa assay in cerebrospinal fluid and blood. *Bioanalysis* **11**, 1405-1418.

[66] Chen JH, Chan L, Chung CC, Bamodu OA, Hong CT (2021) Blood Neurofilament Light Chain in Parkinson's Disease: Comparability between Parkinson's Progression Markers Initiative (PPMI) and Asian Cohorts. *J Clin Med* **10**.

[67] Nagatsua T, Sawadab M (2009) L-dopa therapy for Parkinson's disease: past, present, and future. *Parkinsonism Relat Disord* **15 Suppl 1**, S3-8.

[68] Hindle JV, Martin-Forbes PA, Martyr A, Bastable AJ, Pye KL, Mueller Gathercole VC, Thomas EM, Clare L (2017) The effects of lifelong cognitive lifestyle on executive function in older people with Parkinson's disease. *Int J Geriatr Psychiatry*.

[69] Advocat J, Enticott J, Vandenberg B, Hassed C, Hester J, Russell G (2016) The effects of a mindfulness-based lifestyle program for adults with Parkinson's disease: a mixed methods, wait list controlled randomised control study. *BMC Neurol* **16**, 166.

[70] Kenborg L, Lassen CF, Ritz B, Andersen KK, Christensen J, Schernhammer ES, Hansen J, Wermuth L, Rod NH, Olsen JH (2015) Lifestyle, family history, and risk of idiopathic Parkinson disease: a large Danish case-control study. *Am J Epidemiol* **181**, 808-816.

[71] Fereshtehnejad SM, Lokk J (2014) Orthostatic hypotension in patients with Parkinson's disease and atypical parkinsonism. *Parkinsons Dis* **2014**, 475854.

[72] Foulds PG, Yokota O, Thurston A, Davidson Y, Ahmed Z, Holton J, Thompson JC, Akiyama H, Arai T, Hasegawa M, Gerhard A, Allsop D, Mann DM (2012) Post mortem cerebrospinal fluid alpha-synuclein levels are raised in multiple system atrophy and distinguish this from the other alpha-synucleinopathies, Parkinson's disease and Dementia with Lewy bodies. *Neurobiol Dis* **45**, 188-195.

[73] Foulds PG, Mitchell JD, Parker A, Turner R, Green G, Diggle P, Hasegawa M, Taylor M, Mann D, Allsop D (2011) Phosphorylated α-synuclein can be detected in blood plasma and is potentially a useful biomarker for Parkinson's disease. *FASEB J* **25**, 4127-4137.

[74] van Steenoven I, Majbour NK, Vaikath NN, Berendse HW, van der Flier WM, van de Berg WDJ, Teunissen CE, Lemstra AW, El-Agnaf OMA (2018) alpha-Synuclein species as potential cerebrospinal fluid biomarkers for dementia with lewy bodies. *Mov Disord* **33**, 1724-1733.

[75] Constantinides VC, Majbour NK, Paraskevas GP, Abdi I, Safieh-Garabedian B, Stefanis L, El-Agnaf OM, Kapaki E (2021) Cerebrospinal Fluid alpha-Synuclein Species in Cognitive and Movements Disorders. *Brain Sci* **11**.

[76] Majbour NK, Vaikath NN, van Dijk KD, Ardah MT, Varghese S, Vesterager LB, Montezinho LP, Poole S, Safieh-Garabedian B, Tokuda T, Teunissen CE, Berendse HW,

van de Berg WD, El-Agnaf OM (2016) Oligomeric and phosphorylated alpha-synuclein as potential CSF biomarkers for Parkinson's disease. *Mol Neurodegener* **11**, 7.

[77] Cariulo C, Martufi P, Verani M, Azzollini L, Bruni G, Weiss A, Deguire SM, Lashuel HA, Scaricamazza E, Sancesario GM, Schirinzi T, Mercuri NB, Sancesario G, Caricasole A, Petricca L (2019) Phospho-S129 α-Synuclein Is Present in Human Plasma but Not in Cerebrospinal Fluid as Determined by an Ultrasensitive Immunoassay. *Front Neurosci* **13**, 889.

[78] Magalhaes P, Lashuel HA (2022) Opportunities and challenges of α-synuclein as a potential biomarker for Parkinson's disease and other synucleinopathies. *NPJ Parkinsons Dis* **8**, 93.

[79] Peng C, Gathagan RJ, Covell DJ, Medellin C, Stieber A, Robinson JL, Zhang B, Pitkin RM, Olufemi MF, Luk KC, Trojanowski JQ, Lee VM (2018) Cellular milieu imparts distinct pathological α-synuclein strains in α-synucleinopathies. *Nature* **557**, 558-563.

[80] Hass EW, Sorrentino ZA, Xia Y, Lloyd GM, Trojanowski JQ, Prokop S, Giasson BI (2021) Disease-, region- and cell type specific diversity of α-synuclein carboxy terminal truncations in synucleinopathies. *Acta Neuropathol Commun* **9**, 146.

[81] Moors TE, Mona D, Luehe S, Duran-Pacheco G, Spycher L, Mundigl O, Kaluza K, Huber S, Hug MN, Kremer T, Ritter M, Dziadek S, Dernick G, van de Berg WDJ, Britschgi M (2022) Multi-platform quantitation of α-synuclein human brain proteoforms suggests disease-specific biochemical profiles of synucleinopathies. *Acta Neuropathol Commun* **10**, 82.

[82] Yang Y, Shi Y, Schweighauser M, Zhang X, Kotecha A, Murzin AG, Garringer HJ, Cullinane PW, Saito Y, Foroud T, Warner TT, Hasegawa K, Vidal R, Murayama S,

Revesz T, Ghetti B, Hasegawa M, Lashley T, Scheres SHW, Goedert M (2022) Structures of α-synuclein filaments from human brains with Lewy pathology. *Nature* **610**, 791-795.

[83] Hsiao JT, Purushothuman S, Jensen PH, Halliday GM, Kim WS (2019) Reductions in COQ2 Expression Relate to Reduced ATP Levels in Multiple System Atrophy Brain. *Front Neurosci* **13**, 1187.

[84] Giasson BI, Mabon ME, Duda JE, Montine TJ, Robertson D, Hurtig HI, Lee VM, Trojanowski JQ (2003) Tau and 14-3-3 in glial cytoplasmic inclusions of multiple system atrophy. *Acta Neuropathol* **106**, 243-250.

[85] Homma T, Mochizuki Y, Tobisawa S, Komori T, Isozaki E (2020) Cerebral white matter tau-positive granular glial pathology as a characteristic pathological feature in long survivors of multiple system atrophy. *J Neurol Sci* **416**, 117010.

[86] Hornung S, Dutta S, Bitan G (2020) CNS-Derived Blood Exosomes as a Promising Source of Biomarkers: Opportunities and Challenges. *Front Mol Neurosci* **13**, 38.

[87] Magalhaes P, Lashuel HA (2022) Opportunities and challenges of alpha-synuclein as a potential biomarker for Parkinson's disease and other synucleinopathies. *NPJ Parkinsons Dis* **8**, 93.

[88] Liu C, Cholerton B, Shi M, Ginghina C, Cain KC, Auinger P, Parkinson Study Group DI, Zhang J (2015) CSF tau and tau/Aβ42 predict cognitive decline in Parkinson's disease. *Parkinsonism Relat Disord* **21**, 271-276.

[89] Montine TJ, Shi M, Quinn JF, Peskind ER, Craft S, Ginghina C, Chung KA, Kim H, Galasko DR, Jankovic J, Zabetian CP, Leverenz JB, Zhang J (2010) CSF Aβ(42) and tau in Parkinson's disease with cognitive impairment. *Mov Disord* **25**, 2682-2685.

[90] Blommer J, Pitcher T, Mustapic M, Eren E, Yao PJ, Vreones MP, Pucha KA, Dalrymple-Alford J, Shoorangiz R, Meissner WG, Anderson T, Kapogiannis D (2022) Extracellular vesicle biomarkers for cognitive impairment in Parkinson's disease. *Brain*.

[91] Taha HB, Hornung S, Dutta S, Fenwick L, Lahgui O, Howe K, Elabed N, Del Rosario I, Wong DY, Duarte Folle A, Markovic D, Palma JA, Kang UJ, Alcalay RN, Sklerov M, Kaufmann H, Fogel BL, Bronstein JM, Ritz B, Bitan G (2023) Toward a biomarker panel measured in CNS-originating extracellular vesicles for improved differential diagnosis of Parkinson's disease and multiple system atrophy. *Transl Neurodegener* **12**, 14.

[92] Payton ME, Greenstone MH, Schenker N (2003) Overlapping confidence intervals or standard error intervals: what do they mean in terms of statistical significance? *J Insect Sci* **3**, 34.

[93] Lashuel HA, Mahul-Mellier AL, Novello S, Hegde RN, Jasiqi Y, Altay MF, Donzelli S, DeGuire SM, Burai R, Magalhaes P, Chiki A, Ricci J, Boussouf M, Sadek A, Stoops E, Iseli C, Guex N (2022) Revisiting the specificity and ability of phospho-S129 antibodies to capture alpha-synuclein biochemical and pathological diversity. *NPJ Parkinsons Dis* **8**, 136.

[94] Kellie JF, Higgs RE, Ryder JW, Major A, Beach TG, Adler CH, Merchant K, Knierman MD (2014) Quantitative measurement of intact alpha-synuclein proteoforms from post-mortem control and Parkinson's disease brain tissue by intact protein mass spectrometry. *Sci Rep* **4**, 5797.

[95] Norman M, Ter-Ovanesyan D, Trieu W, Lazarovits R, Kowal EJK, Lee JH, Chen-Plotkin AS, Regev A, Church GM, Walt DR (2021) L1CAM is not associated with extracellular vesicles in human cerebrospinal fluid or plasma. *Nat Methods* **18**, 631-634.

[96] Taha HB, Ati SS (2023) Evaluation of α-Synuclein in CNS-originating Extracellular Vesicles for Parkinsonian Disorders: A Systematic Review and Meta-analysis. *Research Square*.

[97] Zhang X, Takeuchi T, Takeda A, Mochizuki H, Nagai Y (2022) Comparison of serum and plasma as a source of blood extracellular vesicles: Increased levels of platelet-derived particles in serum extracellular vesicle fractions alter content profiles from plasma extracellular vesicle fractions. *PLoS One* **17**, e0270634.

[98] Lacroix R, Judicone C, Poncelet P, Robert S, Arnaud L, Sampol J, Dignat-George F (2012) Impact of pre-analytical parameters on the measurement of circulating microparticles: towards standardization of protocol. *J Thromb Haemost* **10**, 437-446.

[99] Karimi N, Dalirfardouei R, Dias T, Lotvall J, Lasser C (2022) Tetraspanins distinguish separate extracellular vesicle subpopulations in human serum and plasma - Contributions of platelet extracellular vesicles in plasma samples. *J Extracell Vesicles* **11**, e12213.

[100] Palviainen M, Saraswat M, Varga Z, Kitka D, Neuvonen M, Puhka M, Joenvaara S, Renkonen R, Nieuwland R, Takatalo M, Siljander PRM (2020) Extracellular vesicles from human plasma and serum are carriers of extravesicular cargo-Implications for biomarker discovery. *PLoS One* **15**, e0236439.

[101] Jayachandran M, Miller VM, Heit JA, Owen WG (2012) Methodology for isolation, identification and characterization of microvesicles in peripheral blood. *J Immunol Methods* **375**, 207-214.

[102] Baek R, Sondergaard EK, Varming K, Jorgensen MM (2016) The impact of various preanalytical treatments on the phenotype of small extracellular vesicles in blood analyzed by protein microarray. *J Immunol Methods* **438**, 11-20.

[103] György B, Pálóczi K, Kovács A, Barabás E, Bekő G, Várnai K, Pállinger É, Szabó-Taylor K, Szabó TG, Kiss AA, Falus A, Buzás EI (2014) Improved circulating microparticle analysis in acid-citrate dextrose (ACD) anticoagulant tube. *Thromb Res* **133**, 285-292.

[104] Théry C, Witwer KW, Aikawa E, Alcaraz MJ, Anderson JD, Andriantsitohaina R, Antoniou A, Arab T, Archer F, Atkin-Smith GK, Ayre DC, Bach JM, Bachurski D, Baharvand H, Balaj L, Baldacchino S, Bauer NN, Baxter AA, Bebawy M, Beckham C, Bedina Zavec A, Benmoussa A, Berardi AC, Bergese P, Bielska E, Blenkiron C, Bobis-Wozowicz S, Boilard E, Boireau W, Bongiovanni A, Borràs FE, Bosch S, Boulanger CM, Breakefield X, Breglio AM, Brennan M, Brigstock DR, Brisson A, Broekman ML, Bromberg JF, Bryl-Górecka P, Buch S, Buck AH, Burger D, Busatto S, Buschmann D, Bussolati B, Buzás EI, Byrd JB, Camussi G, Carter DR, Caruso S, Chamley LW, Chang YT, Chen C, Chen S, Cheng L, Chin AR, Clayton A, Clerici SP, Cocks A, Cocucci E, Coffey RJ, Cordeiro-da-Silva A, Couch Y, Coumans FA, Coyle B, Crescitelli R, Criado MF, D'Souza-Schorey C, Das S, Datta Chaudhuri A, de Candia P, De Santana EF, De Wever O, Del Portillo HA, Demaret T, Deville S, Devitt A, Dhondt B, Di Vizio D, Dieterich LC, Dolo V, Dominguez Rubio AP, Dominici M, Dourado MR, Driedonks TA, Duarte FV, Duncan HM, Eichenberger RM, Ekström K, El Andaloussi S, Elie-Caille C, Erdbrügger U, Falcón-Pérez JM, Fatima F, Fish JE, Flores-Bellver M, Försönits A, Frelet-Barrand A, Fricke F, Fuhrmann G, Gabrielsson S, Gámez-Valero A, Gardiner C, Gärtner K, Gaudin R, Gho YS, Giebel B, Gilbert C, Gimona M, Giusti I, Goberdhan DC, Görgens A, Gorski SM, Greening DW, Gross JC, Gualerzi A, Gupta GN, Gustafson D, Handberg A, Haraszti RA, Harrison P, Hegyesi H, Hendrix A, Hill AF, Hochberg FH,

Hoffmann KF, Holder B, Holthofer H, Hosseinkhani B, Hu G, Huang Y, Huber V, Hunt S, Ibrahim AG, Ikezu T, Inal JM, Isin M, Ivanova A, Jackson HK, Jacobsen S, Jay SM, Jayachandran M, Jenster G, Jiang L, Johnson SM, Jones JC, Jong A, Jovanovic-Talisman T, Jung S, Kalluri R, Kano SI, Kaur S, Kawamura Y, Keller ET, Khamari D, Khomyakova E, Khvorova A, Kierulf P, Kim KP, Kislinger T, Klingeborn M, Klinke DJ, Kornek M, Kosanović MM, Kovács Á, Krämer-Albers EM, Krasemann S, Krause M, Kurochkin IV, Kusuma GD, Kuypers S, Laitinen S, Langevin SM, Languino LR, Lannigan J, Lässer C, Laurent LC, Lavieu G, Lázaro-Ibáñez E, Le Lay S, Lee MS, Lee YXF, Lemos DS, Lenassi M, Leszczynska A, Li IT, Liao K, Libregts SF, Ligeti E, Lim R, Lim SK, Linē A, Linnemannstöns K, Llorente A, Lombard CA, Lorenowicz MJ, Lörincz Á, Lötvall J, Lovett J, Lowry MC, Loyer X, Lu Q, Lukomska B, Lunavat TR, Maas SL, Malhi H, Marcilla A, Mariani J, Mariscal J, Martens-Uzunova ES, Martin-Jaular L, Martinez MC, Martins VR, Mathieu M, Mathivanan S, Maugeri M, McGinnis LK, McVey MJ, Meckes DG, Meehan KL, Mertens I, Minciacchi VR, Möller A, Møller Jørgensen M, Morales-Kastresana A, Morhayim J, Mullier F, Muraca M, Musante L, Mussack V, Muth DC, Myburgh KH, Najrana T, Nawaz M, Nazarenko I, Nejsum P, Neri C, Neri T, Nieuwland R, Nimrichter L, Nolan JP, Nolte-'t Hoen EN, Noren Hooten N, O'Driscoll L, O'Grady T, O'Loghlen A, Ochiya T, Olivier M, Ortiz A, Ortiz LA, Osteikoetxea X, Østergaard O, Ostrowski M, Park J, Pegtel DM, Peinado H, Perut F, Pfaffl MW, Phinney DG, Pieters BC, Pink RC, Pisetsky DS, Pogge von Strandmann E, Polakovicova I, Poon IK, Powell BH, Prada I, Pulliam L, Quesenberry P, Radeghieri A, Raffai RL, Raimondo S, Rak J, Ramirez MI, Raposo G, Rayyan MS, Regev-Rudzki N, Ricklefs FL, Robbins PD, Roberts DD, Rodrigues SC, Rohde E, Rome S, Rouschop KM,

Rughetti A, Russell AE, Saá P, Sahoo S, Salas-Huenuleo E, Sánchez C, Saugstad JA, Saul MJ, Schiffelers RM, Schneider R, Schøyen TH, Scott A, Shahaj E, Sharma S, Shatnyeva O, Shekari F, Shelke GV, Shetty AK, Shiba K, Siljander PR, Silva AM, Skowronek A, Snyder OL, Soares RP, Sódar BW, Soekmadji C, Sotillo J, Stahl PD, Stoorvogel W, Stott SL, Strasser EF, Swift S, Tahara H, Tewari M, Timms K, Tiwari S, Tixeira R, Tkach M, Toh WS, Tomasini R, Torrecilhas AC, Tosar JP, Toxavidis V, Urbanelli L, Vader P, van Balkom BW, van der Grein SG, Van Deun J, van Herwijnen MJ, Van Keuren-Jensen K, van Niel G, van Royen ME, van Wijnen AJ, Vasconcelos MH, Vechetti IJ, Veit TD, Vella LJ, Velot É, Verweij FJ, Vestad B, Viñas JL, Visnovitz T, Vukman KV, Wahlgren J, Watson DC, Wauben MH, Weaver A, Webber JP, Weber V, Wehman AM, Weiss DJ, Welsh JA, Wendt S, Wheelock AM, Wiener Z, Witte L, Wolfram J, Xagorari A, Xander P, Xu J, Yan X, Yáñez-Mó M, Yin H, Yuana Y, Zappulli V, Zarubova J, Žėkas V, Zhang JY, Zhao Z, Zheng L, Zheutlin AR, Zickler AM, Zimmermann P, Zivkovic AM, Zocco D, Zuba-Surma EK (2018) Minimal information for studies of extracellular vesicles 2018 (MISEV2018): a position statement of the International Society for Extracellular Vesicles and update of the MISEV2014 guidelines. *J Extracell Vesicles* **7**, 1535750.

[105] Gomes DE, Witwer KW (2022) L1CAM-associated extracellular vesicles: A systematic review of nomenclature, sources, separation, and characterization. *J Extracell Biol* **1**.

[106] Clayton A, Boilard E, Buzas EI, Cheng L, Falcon-Perez JM, Gardiner C, Gustafson D, Gualerzi A, Hendrix A, Hoffman A, Jones J, Lasser C, Lawson C, Lenassi M, Nazarenko I, O'Driscoll L, Pink R, Siljander PR, Soekmadji C, Wauben M, Welsh JA, Witwer K,

Zheng L, Nieuwland R (2019) Considerations towards a roadmap for collection, handling and storage of blood extracellular vesicles. *J Extracell Vesicles* **8**, 1647027.

[107] Dutta S, Hornung S, Taha HB, Bitan G (2023) Biomarkers for parkinsonian disorders in CNS-originating EVs: promise and challenges. *Acta Neuropathol*, 1-26.

[108] Yu Z, Shi M, Stewart T, Fernagut PO, Huang Y, Tian C, Dehay B, Atik A, Yang D, De Giorgi F, Ichas F, Canron MH, Ceravolo R, Frosini D, Kim HJ, Feng T, Meissner WG, Zhang J (2020) Reduced oligodendrocyte exosome secretion in multiple system atrophy involves SNARE dysfunction. *Brain* **143**, 1780-1797.

[109] Shi M, Liu C, Cook TJ, Bullock KM, Zhao Y, Ginghina C, Li Y, Aro P, Dator R, He C, Hipp MJ, Zabetian CP, Peskind ER, Hu SC, Quinn JF, Galasko DR, Banks WA, Zhang J (2014) Plasma exosomal α-synuclein is likely CNS-derived and increased in Parkinson's disease. *Acta Neuropathol* **128**, 639-650.

[110] Zhao ZH, Chen ZT, Zhou RL, Zhang X, Ye QY, Wang YZ (2019) Increased DJ-1 and α-synuclein in plasma neural-derived exosomes as potential markers for Parkinson's disease. *Frontiers in Aging Neuroscience* **11**.

[111] Zou J, Guo Y, Wei L, Yu F, Yu B, Xu A (2020) Long Noncoding RNA POU3F3 and alpha-Synuclein in Plasma L1CAM Exosomes Combined with beta-Glucocerebrosidase Activity: Potential Predictors of Parkinson's Disease. *Neurotherapeutics* **17**, 1104-1119.

[112] Blommer J, Pitcher T, Mustapic M, Eren E, Yao PJ, Vreones MP, Pucha KA, Dalrymple-Alford J, Shoorangiz R, Meissner WG, Anderson T, Kapogiannis D (2023) Extracellular vesicle biomarkers for cognitive impairment in Parkinson's disease. *Brain* **146**, 195-208.

[113] Si X, Tian J, Chen Y, Yan Y, Pu J, Zhang B (2019) Central Nervous System-Derived Exosomal Alpha-Synuclein in Serum May Be a Biomarker in Parkinson's Disease. *Neuroscience* **413**, 308-316.

[114] Jiang C, Hopfner F, Berg D, Hu MT, Pilotto A, Borroni B, Davis JJ, Tofaris GK (2021) Validation of α-Synuclein in L1CAM-Immunocaptured Exosomes as a Biomarker for the Stratification of Parkinsonian Syndromes. *Mov Disord* **36**, 2663-2669.

[115] Jiang C, Hopfner F, Katsikoudi A, Hein R, Catli C, Evetts S, Huang Y, Wang H, Ryder JW, Kuhlenbaeumer G, Deuschl G, Padovani A, Berg D, Borroni B, Hu MT, Davis JJ, Tofaris GK (2020) Serum neuronal exosomes predict and differentiate Parkinson's disease from atypical parkinsonism. *J Neurol Neurosurg Psychiatry* **91**, 720-729.

[116] Consortium E-T, Van Deun J, Mestdagh P, Agostinis P, Akay O, Anand S, Anckaert J, Martinez ZA, Baetens T, Beghein E, Bertier L, Berx G, Boere J, Boukouris S, Bremer M, Buschmann D, Byrd JB, Casert C, Cheng L, Cmoch A, Daveloose D, De Smedt E, Demirsoy S, Depoorter V, Dhondt B, Driedonks TA, Dudek A, Elsharawy A, Floris I, Foers AD, Gartner K, Garg AD, Geeurickx E, Gettemans J, Ghazavi F, Giebel B, Kormelink TG, Hancock G, Helsmoortel H, Hill AF, Hyenne V, Kalra H, Kim D, Kowal J, Kraemer S, Leidinger P, Leonelli C, Liang Y, Lippens L, Liu S, Lo Cicero A, Martin S, Mathivanan S, Mathiyalagan P, Matusek T, Milani G, Monguio-Tortajada M, Mus LM, Muth DC, Nemeth A, Nolte-'t Hoen EN, O'Driscoll L, Palmulli R, Pfaffl MW, Primdal-Bengtson B, Romano E, Rousseau Q, Sahoo S, Sampaio N, Samuel M, Scicluna B, Soen B, Steels A, Swinnen JV, Takatalo M, Thaminy S, Thery C, Tulkens J, Van Audenhove I, van der Grein S, Van Goethem A, van Herwijnen MJ, Van Niel G, Van Roy N, Van Vliet AR, Vandamme N, Vanhauwaert S, Vergauwen G, Verweij F, Wallaert A, Wauben M,

Witwer KW, Zonneveld MI, De Wever O, Vandesompele J, Hendrix A (2017) EV-TRACK: transparent reporting and centralizing knowledge in extracellular vesicle research. *Nat Methods* **14**, 228-232.

[117] Dutta S, Hornung S, Taha HB, Biggs K, Siddique I, Chamoun LM, Shahpasand-Kroner H, Lantz C, Herrera-Vaquero M, Stefanova N, Loo JA, Bitan G (2023) Development of a Novel Electrochemiluminescence ELISA for Quantification of α-Synuclein Phosphorylated at Ser. *ACS Chem Neurosci*.

[118] Shahnawaz M, Mukherjee A, Pritzkow S, Mendez N, Rabadia P, Liu X, Hu B, Schmeichel A, Singer W, Wu G, Tsai AL, Shirani H, Nilsson KPR, Low PA, Soto C (2020) Discriminating α-synuclein strains in Parkinson's disease and multiple system atrophy. *Nature* **578**, 273-277.

[119] Barbagallo C, Mostile G, Baglieri G, Giunta F, Luca A, Raciti L, Zappia M, Purrello M, Ragusa M, Nicoletti A (2020) Specific Signatures of Serum miRNAs as Potential Biomarkers to Discriminate Clinically Similar Neurodegenerative and Vascular-Related Diseases. *Cell Mol Neurobiol* **40**, 531-546.

[120] Yao YF, Qu MW, Li GC, Zhang FB, Rui HC (2018) Circulating exosomal miRNAs as diagnostic biomarkers in Parkinson's disease. *Eur Rev Med Pharmacol Sci* **22**, 5278-5283.

[121] Cao XY, Lu JM, Zhao ZQ, Li MC, Lu T, An XS, Xue LJ (2017) MicroRNA biomarkers of Parkinson's disease in serum exosome-like microvesicles. *Neurosci Lett*.

[122] Rani A, O'Shea A, Ianov L, Cohen RA, Woods AJ, Foster TC (2017) miRNA in Circulating Microvesicles as Biomarkers for Age-Related Cognitive Decline. *Front Aging Neurosci* **9**, 323.

[123] Gui Y, Liu H, Zhang L, Lv W, Hu X (2015) Altered microRNA profiles in cerebrospinal fluid exosome in Parkinson disease and Alzheimer disease. *Oncotarget* **6**, 37043-37053.

[124] Blondal T, Jensby Nielsen S, Baker A, Andreasen D, Mouritzen P, Wrang Teilum M, Dahlsveen IK (2013) Assessing sample and miRNA profile quality in serum and plasma or other biofluids. *Methods* **59**, S1-6.

[125] Lawton M, Kasten M, May MT, Mollenhauer B, Schaumburg M, Liepelt-Scarfone I, Maetzler W, Vollstedt EJ, Hu MT, Berg D, Ben-Shlomo Y (2016) Validation of conversion between mini-mental state examination and montreal cognitive assessment. *Mov Disord* **31**, 593-596.

Epilogue

In Chapter 1, the research underscored the urgent need for a reliable and robust assay to detect and measure pS129-α-synuclein (pS129-α-syn). α-Synuclein (α-syn) is a protein that is thought to function in pre-synaptic vesicle release, however, when mutated or dysfunctional, clumps together to form Lewy bodies, aggregates found in the neurons of patients with Parkinson's Disease (PD) and other synucleinopathies such as Multiple System Atrophy (MSA). A phosphorylated form of this protein, pS129-α-syn, is considered a hallmark of these diseases and is significantly increased in α-syn aggregates found in postmortem studies.

This highlights the importance of an assay that can accurately quantify pS129-α-syn, particularly if it could be derived from easily accessible body fluids such as blood or cerebrospinal fluid. Such an assay, which is not currently commercially available, may enable non-invasive monitoring of disease progression, early detection, and evaluation of therapeutic efficacy in clinical trials. It could also contribute to personalized treatment planning, thereby improving the overall management of these neurodegenerative diseases. Therefore, the focus of Chapter 1 was to develop and characterize such an assay.

Building upon this necessity, Chapter 2 utilized this assay to measure pS129-α-syn in neuronal and oligodendroglial extracellular vesicles (nEVs and oEVs, respectively). Extracellular vesicles (EVs), which include nEVs and oEVs, are tiny particles released by cells. They carry a variety of cellular components, including proteins, lipids, and nucleic acids, mirroring their parent cell's status. As a result, these vesicles are considered promising candidates as potential biomarkers for a variety of diseases, including neurodegenerative disorders.

Previously, it was shown that the oEVs:nEVs α-syn ratio is >1 in most patients with MSA while <1 in most patients with PD. Building on these results, Chapter 2 aimed to investigate whether the addition of nEV/oEV pS129-α-syn, along with other biomarkers such as total tau, pTau181-tau, and serum/plasma neurofilament light chain (NfL), could improve the diagnostic power among patients with PD, MSA, and healthy controls (HCs).

The study discovered that the inclusion of oEV pS129-α-syn may improve the predictive differentiation among these groups. It was noted that although tau concentrations were significantly lower in MSA than in HC or PD in both nEVs and oEVs, they did not enhance prediction accuracy. Although NfL alone did not enhance the group separation, when added to the model with oEV tau, it improved the differentiation between the HC and PD groups, but not between PD and MSA, which is more clinically relevant.

Despite these promising findings, I also highlighted some significant limitations and critical points for consideration. One of the major issues is the assay matrix effect that may exist in the developed pS129-α-syn assay. Other research groups attempting to replicate some of the previous findings were not successful, which raises questions about experimental reproducibility or potential methodology issues of using CNS-originating EVs. Additionally, there were some discrepancies between neuropathological diagnoses obtained postmortem and those obtained premortem, which cast doubts on the reliability of premortem diagnostic accuracy.

Furthermore, the study's findings were not independently validated, thus weakening their overall impact and generalizability. Other critical points include the issues with possible antibody cross-reactivity as well as whether the isolated nEVs and oEVs do indeed originate from the brain. Most importantly, control of preanalytical variables that are known to affect the EV signature were not controlled for during the study, which weakens the results. These limitations highlight the critical need for further studies with larger cohorts and independent validation to consolidate these initial findings and help establish a more robust understanding of these biomarkers' potential.

Efforts are ongoing, particularly by the International Society for Extracellular Vesicles (ISEV) and other bodies, to achieve more rigorous standardization of methodologies used in EV research. This could increase the chances of successful replication of findings and help build a more reliable database of EV-associated biomarkers. Finally, while our study focused on patients with PD and MSA only, other diseases such as Lewy Body Dementia, Progressive Supranuclear Palsy, and Corticobasal Syndrome may be fruitful to include in future studies.